Aus dem Institut für Neuroradiologie

der Universität zu Lübeck

Direktor: Prof. Dr. med. Peter Schramm

EVALUATING THE GLYMPHATIC SYSTEM VIA MAGNETIC RESONANCE DIFFUSION-TENSOR IMAGING ALONG THE PERIVASCULAR SPACES IN BRAIN TUMOR PATIENTS

Inauguraldissertation
zur Erlangung der Doktorwürde
der Universität zu Lübeck
- Aus der Sektion Medizin -

Vorgelegt von
Maria Gabriela Villacis Miranda
aus GUAYAQUIL / ECUADOR
Lübeck 2025

1. Berichterstatter: Prof. Dr. med. Peter Schramm
Kobetreuer: PD. Dr. med. Jan Küchler
2. Berichterstatter: PD Dr. sc. Ana Westenberger
Tag der mündlichen Prüfung: 09.09.2025
Zum Druck genehmigt. Lübeck, den 22.09.2025
-Promotionskomission der Sektion Medizin-

Die Ergebnisse dieser Arbeit wurden bereits publiziert:

Villacis G, Schmidt A, Rudolf JC, Schwenke H, Küchler J, Schramm P, Ulloa P. Evaluating the glymphatic system via magnetic resonance diffusion tensor imaging along the perivascular spaces in brain tumor patients. *Jpn J Radiol.* 42, 1146–1156 (2024) doi: 10.1007/s11604-024-01602-7

To my husband and my son,
sources of support and inspiration

Table of Contents

List of Figures

List of Tables

1 Introduction

Researchers long wondered why the brain, which has a very high metabolic rate and takes about one fifth of the total body oxygen consumption[1], did not have a lymphatic connection or seem to have a system for waste clearance. Over the years, many theories have been developed on how the brain disposes of waste. One such theory, the intramural periarterial drainage (IPAD) theory[2], suggests that waste products are cleared by the cerebrospinal fluid (CSF) entering the cerebral cortex along the pial-glial basement membranes due to the lack of perivascular space around arteries[2]. In this system, the CSF exits along the smooth muscle cell basement membranes[3]. Another theory suggests that lymphatic vessels in the meningeal sheath are used to drain the CSF that has accumulated in the brain tissue[4,5]; a third one posits that the CSF is reabsorbed through the arachnoid granulations.

Most likely, waste management in the brain is the result of complementary pathways working together. However, one theory is considered to be extremely promising: the glymphatic system. Research into this theory has provided an explanation for a long-asked question, with a simple answer: a highly organized system.

1.1 The glymphatic system

The glymphatic system was recently proposed as an important factor in the waste clearance system of the brain[6]. In the human body, from the neck down, we have the lymphatic system. This system carries lymph from the extracellular spaces through the large veins back into the body circulation. By doing this, it also rids metabolic waste products from the system.

In 2012, Iliff et al.[7] used two photon imaging and fluorescent tracers in the brains of mice with in vivo magnetic resonance imaging (MRI) and demonstrated how CSF flows from the arterial vessels through the interstitial space and along the venous perivascular spaces[8]. This fluid is later collected, passes through the

meningeal lymph vessels[9,10], and is reintroduced to the cervical lymph nodes[7,11,12]. It is thought that solutes are distributed in the interstitial space through the movement of CSF into the parenchyma[6].

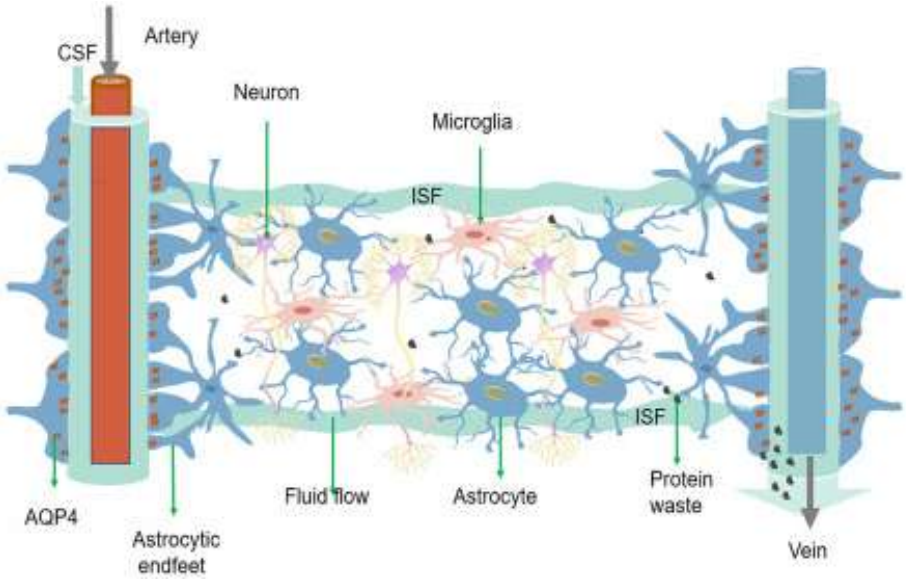

Figure 1 Visualization of glymphatic system. The flow of cerebrospinal fluid (CSF) is mediated through aquaporins 4 (AQ4), from the arterial end, through the parenchyma into the perivenous spaces. Licensed under Creative Commons (CC BY), Ren et al.[13]

Pulsation of the arteries drives movement of the CSF[14], which creates pressure waves and pushes the interstitial fluid in the direction of the veins, like shown in Fig. 1. Respiration[11,15], placement of the head, and the production of CSF are also important aspects here. It has also been shown that, in mice, sleep is a leading influential factor, as well as the position, being more effective in the lateral position[16]. A parallel has been extended to humans.

This system is dependent on aquaporin 4 (AQ4), which is found in the feet of the astrocytes that, together with the arterioles, constitute the blood--brain barrier (BBB). Iliff et al.[7] showed that the CSF flow slowed down and that solutes were not cleared as effectively in mice without AQ4 as in mice with functioning AQ4.

Furthermore, it has been shown that a decrease in glymphatic system function could lead to accumulation of waste products, for example, amyloid ß[6]. This

could be an important factor in the development of diseases such as Alzheimer´s disease[17], normal pressure hydrocephalus[18,19], Parkinson´s disease[20], and others.

In recent years, many studies have dealt with this hypothesis, taking into consideration the practical limitations of the method. The studies of Iliff et al.[7,14,21] were rather invasive, requiring intrathecal injection of a radioactive tracer, which does come with considerable potential for complications. This approach restricts the possibility of widespread use for diagnostic purposes as major life-threatening complications have been observed and it remains an off-label use[22] in humans.

Subsequently, noninvasive methods to evaluate the glymphatic system function are needed. The use of imaging, be it computed tomography (CT) or MRI, represents a natural choice. It is already widespread and in use for diagnostic purposes. The remaining considerations are associated with the quality of the images and the use of ionizing radiation. MRI utilizes magnets and the signal from water molecules and, if needed, an exogenous contrast agent, but without radiation, to produce high-definition images while being minimally invasive. Here, the noninvasive technique of diffusion-tensor imaging (DTI) MRI has been utilized.

Taoka et al.[23] proposed the DTI along perivascular spaces (DTI ALPS) index as a diffusivity ratio, which represents water diffusion along the perivascular spaces using the strategic position of the medullary veins. Using this index, we can analyze diffusivity along the perivascular space[24] and estimate the function of the glymphatic system.

Therefore, several researchers have investigated the glymphatic system using the movement of water in the white matter[20,25]. According to their theory, the movement of water along the perpendicular periventricular veins could serve to evaluate glymphatic function in the human brain. The practical applications of the DTI ALPS index in this case could extend from early biomarker for neurodegenerative diseases to screening for early detection of cancerous developments that cannot yet be seen in normal scans.

In the present thesis, I use the DTI ALPS index to assess the function of the glymphatic system in patients with different kinds of brain tumors and compare it to healthy controls (HCs). To further examine the underlying mechanism and build up my current research, it is necessary to give an overview of the anatomy.

1.2 Brain microstructure

The nervous system is divided into the central and peripheral nervous system. The central nervous system (CNS) is composed of the spine and the brain. Both structures can be divided into white and gray matter. The gray matter contains the cell bodies of the neurons, the white matter mostly myelin-wrapped axons. In the brain, the gray matter is found in the outer layer, the cortex, while the white matter lies in the deeper layers. The nuclei, embedded in the white matter, are the exception. In the cortex and nuclei, we find the bodies of the neurons.

The neurons are supported by glial cells. Histologically and functionally, they have been divided into astrocytes, oligodendrocytes, microglia, and ependymal cells. This microstructure forms the basis of the glymphatic system because the astrocytes compose the border to the neuropil.

Oligodendrocytes build the myelin sheath by wrapping their feet around the axons. The microglia constitute the macrophages of the CNS and are part of the monocytic phagocytic system. The ependymal cells line the cerebral ventricles and the spinal cord.

Astrocytes represent the largest and most common of the four kinds of cells. They are found in both the gray matter as protoplasmic cells and in the white matter as fibrillar cells. With their feet they build the BBB with small arterial vessels. As these vessels do not have a tunica media, the astrocytic feet are only separated from the vessels and their cells through the basal membrane. This induces the tight junctions in the astrocytic feet and gives the BBB its characteristic impermeability[26]. The impermeability is mediated by AQ4, located on the astrocytic feet, which allows the flow of CSF into the neuropil. This ability also forms the basis of the theory of the glymphatic system.

Like all cells, glial cells can degenerate into benign or malignant cells, forming tumors. Depending on their location, these tumors can cause different symptoms.

1.3 Brain tumors

Brain tumors are among the 10 most common diseases of the CNS. A study from 2020 analyzed the different neurological diseases and their frequency in western Europe and the world[27]. Brain tumors and nervous system cancer ranked 9th, with a prevalence in Europe of 45 in 100,000 and an incidence of 9 per 100,000[27]. They are interesting to study due to the mortality associated with them, resulting in 143 per 100,000 years of life lost and 4 per 100,000 years lived with the disease in 2017[27].

Tumors can be classified according to the origin of the degenerated tissue, where primary brain tumors are defined as those from tissue found in the CNS. They can be benign or malignant, whereas secondary tumors originate in other tissues in the body. Secondary tumors are more common than primary tumors, develop about four times more often[28], and are always malignant.

The predominant, primary intra-axial tumors derive from astrocytes. Glioblastoma is the most common one, with an incidence of 6 in 100,000, and becomes manifest at an average age of 56 years[29]. To define a tumor as such, one of the following criteria must be fulfilled: microvascular proliferation or necrosis or *TERT* promotor mutation or *EGFR* gene amplification or +7/–10 chromosome copy number changes. This tumor is one of the adult-type diffuse gliomas and is graded from 2 to 4 within its type[30]. It would typically be hypointense on the MRIT1-weighted images and hyperintense on T2-weighted images, with edema.

The isocitrate dehydrogenase (IDH) mutant astrocytoma is also an adult-type diffuse astrocytoma with a prevalence of 2-3 cases in 100,000, becoming manifest at an average age of 46 years. This tumor would typically show homogeneity of the mass with a relatively hypointense signal throughout most of the lesion on FLAIR sequences as compared to T2-weighted images except for a peripheral rim of hyperintense signal.

Other glial tumors occur at a much lower frequency, such as oligodendrogliomas. Their incidence is roughly 0.5-1 in 100,000 presenting at an average age of 40 years[29]. They can be IDH mutant and 1p/19q-codeleted, with or without calcifications and variable enhancement on images.

Extra-axially, we frequently find meningiomas. This kind of tumor is the second most common primary tumor, with an incidence of approximately 5 in 100,000[29], presenting at an average age of 60 years. They tend to grow slowly and can be treated, having the best survival rate at 90% after 5 years[29]. Early diagnosis can open up more options to treat the tumor.

Certain kinds of tumors metastasize most frequently to the CNS. Lung cancer, breast cancer, and melanoma[28] are at the top of the list here. Brain metastases usually occur in the cerebral hemispheres, supra- or infratentorially. Once a metastasis is found in the brain, it usually means that a systemic disease is well advanced. If metastasis constitutes the first presentation of the disease, a biopsy will help to determine tumor histology. Subsequently, the search for the primary tumor will begin, which, in cases of melanoma, for example, is not always easy.

Symptoms depend on the size and location of the tumor. They can range from focal neurological deficits, seizures, and diffuse headaches to changes in personality or behavior, among others. Once symptoms are present, the first diagnostic step after anamnesis and examination of the patient, is head imaging. The gold standard here is MRI with and without contrast agent. Depending on the symptoms and the availability of a MR scanner, in acute cases, contrast-enhanced CT can also be used.

Further strategies are then decided in a multidisciplinary setting involving neurologists, neurooncologists, neurosurgeons, neuroradiologists, and radiotherapists, for each patient individually. The treatment can encompass surgery, chemotherapy, and radiotherapy.

In earlier years, imaging was used to diagnose tumors, depending on certain characteristics, for example, the presence of necrosis, high vascularization, or cysts. These findings, in combination with a biopsy, would lead to the diagnosis. This approach has been revised for brain tumors in the new version of the WHO Tumor Classification System.

1.4 WHO Tumor Classification System

The WHO Classification, 5th edition (CNS5), catalogs brain tumors depending on their histologic features and genetic mutations[30]. In this edition, CNS neoplasms are sorted into the categories gliomas and glioneuronal and neuronal tumors; choroid plexus tumors; embryonal tumors; pineal tumors; cranial and paraspinal nerve tumors; meningioma; mesenchymal, nonmeningothelial tumors; melanocytic tumors; hematolymphoid tumors; germ cell tumors; tumors of the sellar region; and metastases to the CNS[31].

The subtypes are classified according to genetic mutations and the patient group. For example, for gliomas, glioneuronal tumors, and neuronal tumors, it is no longer sufficient to characterize the tumor´s genetic markers for IDH1 and IDH2. Further genetic markers need to be examined, depending on the tumor, its characteristics, and the patient. This has resulted in a new classification form that rates the stages from 1 to 4, taking into consideration that it neither fully encompasses the treatment possibilities, which could well prolong the survival of the patient, nor the full morphology, such as necrosis or blood vessel development.

The CNS5 also uses the abbreviations “Not otherwise specified (NOS)” and “not elsewhere classified (NEC)” to label the global diagnosis if the tumors cannot be clearly defined.

Indeed, genetic characterization of tumors opens up possibilities for new approaches to treatment, such as tumor-targeting antibodies or, in the case of glioblastoma, even oncolysis[32].

1.5 MRI and diffusion-weighted imaging

1.5.1 Basics of MRI

The MRI technique is based on the physical principle that nuclei with spins align when placed in a magnetic field. MRI takes advantage of the fact that hydrogen is the most abundant atom in human beings. This is very convenient because hydrogen protons have a property called spin, which is fundamental for the concept of resonance[33].

Once put in a magnetic field, such as in an MRI scanner, the atoms will align. This alignment is either parallel or antiparallel to the magnetic field. As spins tend to seek the lower energy levels, more spins are aligned parallel than anti-parallel to the magnetic field. How many align on each direction depends on the strength of the magnetic field. Adding parallel and anti-parallel spins is called net magnetization. Net magnetization is a vector (has a magnitude and a direction) in the x´-y´-z´ plane.

Using a radiofrequency (RF) impulse, the net magnetization vector is flipped by an angle alpha, which is usually 90 degrees. Once the RF impulse stops, the protons strive to return to their state of lower energy in both the z (T1 relaxation time) and x-y (T2 relaxation time) planes. They are separate, but simultaneous processes, which also take place at different speeds. T1 is slower than T2, taking up to seconds, while T2 takes tens of milliseconds. This depends on the tissue properties of the site where the protons are. The relaxation process emits a RF signal, which is received by a coil and transduced by the system, and then the computer can construct an image.

The basic contrast of an MR image depends on the density of protons in the tissue and the relaxation times (T1 and T2). In the T1-weighted images, tissues with a short T1 relaxation time (e.g., fat) appear hyperintense. On the other hand, tissues with a longer T1 relaxation time (e.g., water) produce a lower signal and are dark in the final image, providing great anatomical detail.

For the T2-weighted contrast, short T2 tissues (e.g., fat) will appear darker, while long T2 (like water) are hyperintense. These images are helpful in identifying

pathological processes, highlighting inflammation or edema due to more water content.

Therefore, MRI is a powerful tool for noninvasive imaging, especially for soft-tissue diagnostic examinations. It is the gold standard in CNS tumor diagnostics, due to the high quality of the soft-tissue images[34].

In this thesis I work with diffusion-weighted imaging (DWI).

1.5.2 Diffusion-weighted MRI

Diffusion-weighted (DW) MRI is a technique based on detecting the Brownian movement of water in the body[35] Brownian movement means that molecules disperse randomly, taken by the energy of the repulsion with other atoms, depending on solutes and temperature. When there is a higher concentration of solutes in a space, water tends to go in that direction to dilute the solutes and reach equilibrium. The random movement of molecules is restricted in the body by the cells; therefore, the diffusion of molecules depends on the microstructure of the tissue.

In DWI, the MRI signal depends on the characteristics of the tissue. In tissues where diffusion is high, the image with show a lower signal, meaning that the signal loss is higher due to diffusion. In free water, for example, in the ventricles, the DWI signal will be lower than when the water movement is restricting in a certain direction: in the white matter, due to the membranes of the axons. Depending on the direction of the movement, contrast is stronger or weaker, as seen in Fig. 2 For clinical evaluation, the average of the movement in the x-y-z directions is taken, which is known as mean diffusivity. In MRI it is also possible to calculate the apparent diffusion coefficient per voxel (ADC), which gives an average of the diffusion in a voxel in the form of a map, see Fig. 3.

This has interesting clinical applications, for example, in cases of stroke or tumor, in which increased cellularity and structural changes reduce or increase ADC, depending on the pathological processes. It is also a powerful tool for defining brain lesions, for example, to differentiate between a cyst, tumor necrosis, and an invasive tumor [36].

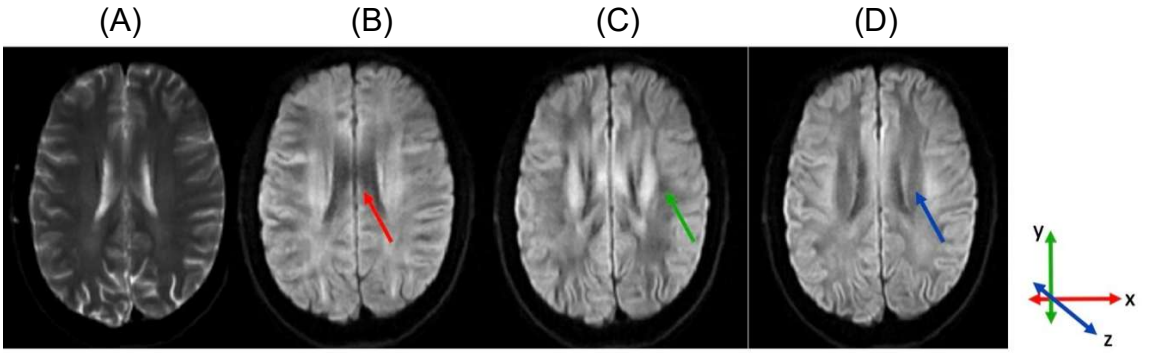

Figure 2 Diffusion-weighted images (DWI) from a healthy volunteer (male, 23 years) using b = 1000 s/mm². (A) Non-diffusion-weighted image (b-value = 0). (B) Diffusion weighting encoded in the x-direction (please note that the corpus callosum shows a low signal, indicating high diffusion along the fibers, in red). (C) Diffusion weighting encoded in the y-direction (please note low signal in longitudinal fasciculus superior, in green). (D) Diffusion weighting encoded in the z-direction (please note low signal in the corona radiata, indicating high diffusion along the fibers, blue arrow). The x-axis corresponds to a left–right direction, the y-axis is anterior-posterior, and the z-axis is head to feet. Low intensity in DWI in the ventricles in the three directions indicates free diffusion.

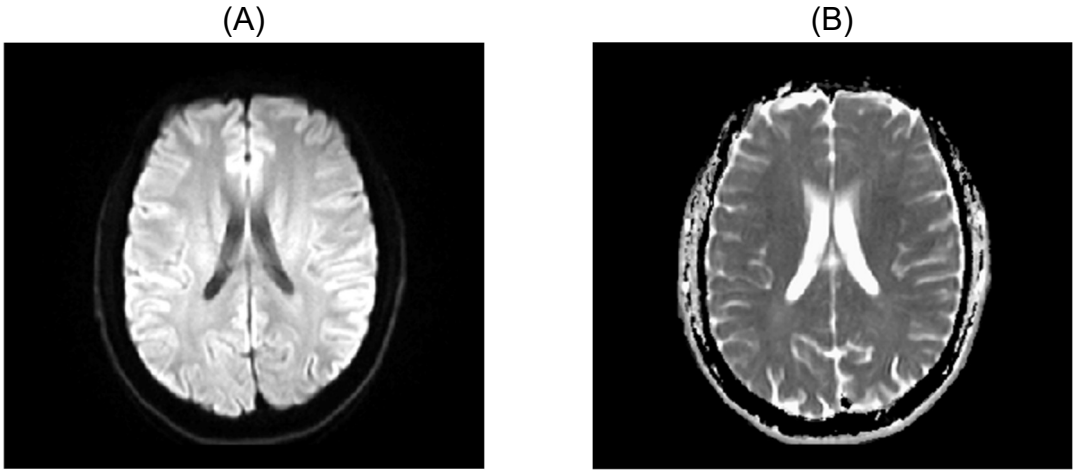

Figure 3 Diffusion-weighted imaging (DWI)-derived maps. Healthy volunteer, male 23 years old. (A) DWI trace, which correspond to the average of the x-, y-, and z- directions and represents the average degree of signal lost due to water diffusion. This results in an image with a contrast that does not depend on the diffusion directions (isotropic). (B) Apparent diffusion coefficient map, calculated using the trace image.

It can also be helpful in characterizing a tumor, considering that malignant tumors tend to have a higher cellularity, which in turn would give a different signal on DWI and ADC. Other characteristics, such as infiltration of the surrounding tissue, necrotic areas, vascularization, and the displacement of healthy brain tissue, are no longer the most important criteria for the profiling and staging of brain tumors. However, the definition of these qualities can provide a roadmap for the direction in which the diagnostic examination should progress.

1.5.3 Diffusion-tensor imaging

In DWI three perpendicular directions are usually used. However, when more than six diffusion encodings are applied, a diffusion tensor can be calculated[37]. Accordingly, we can calculate the directional movement of water. Fractional anisotropy (FA) is a parameter that can be calculated by DTI, with values ranging from 0 to 1, and can evaluate directionality of water in the brain: low FA means isotropic molecular movement (like water in the ventricles) and when movement is mostly in one direction FA is close to 1.

1.5.4 Diffusion-tensor imaging along perivascular spaces

CSF is present in and can move along the perivascular spaces. We can adjust the DTI measurements to detect any movement and quantify it. Accumulation of metabolic waste, misfolded proteins, and fluid, among other products, in the perivascular space could influence and hinder CSF dynamics there and impair function of the brain. DTI ALPS is a promising noninvasive technique developed by Taoka et al.[24,38] to evaluate the glymphatic system function. Here, an index is generated as a diffusivity ratio that represents water diffusion along the perivascular spaces of the medullary veins. These veins were chosen because of their anatomical position, lying perpendicular to the ventricle wall and parallel to each other, as well as their anatomical consistency. The perivascular spaces run parallel to the veins, meaning in a right-to-left direction. In this plane we have the superior longitudinal fascicles and projection fibers running perpendicular from the medullary veins and their perivascular spaces, in the anterior-posterior and head-to-foot

directions, respectively, while the cortical fibers run parallel, right-to-left, as seen in Fig. 4.

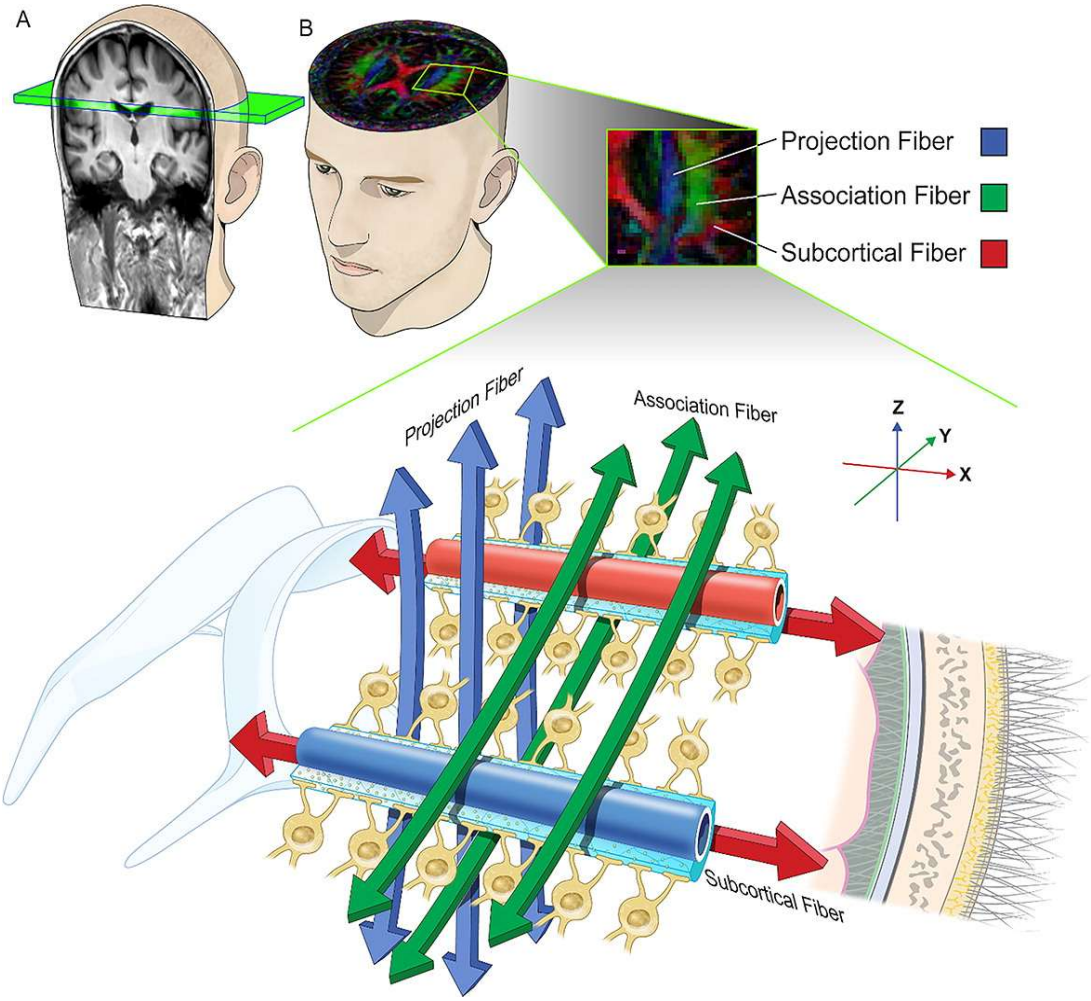

Figure 4 Schematic illustration of the principle underlying the diffusion-tensor imaging analysis along the perivascular space (DTI ALPS) method. (A) At the lateral ventricular body level, the neural fibers are identified on a (B) color-coded fractional anisotropy map. Perivascular water flows perpendicular to projection and association neural fibers. Therefore, diffusivity along the x-axis at these areas mostly reflects perivascular glymphatic flows. Figure from Bae, et al[56]. Permission obtained from the Copyright Clearance Center (CCC), license number: 1477524-1

Calculating the DTI ALPS index could be applied effectively for understanding the function of the glymphatic system. It has been proposed that improper function of this system and the accumulation of metabolic waste, misfolded proteins, or fluid, for example, could influence brain function and play an important role in the

development of many diseases. One could also compare the DTI ALPS index in patients with neurodegenerative diseases and compare it to values in healthy control. as decreases in the DTI ALPS index have been reported in said diseases. This index has been used in many studies as a measure of glymphatic system function, such as in Parkinson´s disease[20,39–45], Alzheimer´s disease[24,46–48], stroke[49], and epilepsy[50–53], where a lower DTI ALPS index might be associated with impaired glymphatic function[7,21]. Importantly, in hydrocephalus patients, this index has shown to be significantly reduced, pointing to glymphatic system dysfunction, as demonstrated by delayed clearance of intrathecally administrated gadobutrol[54,55]. Other risk factors are also being studied, for example, arteriosclerosis and age.

Therefore, the DTI ALPS index appears to be a new biomarker for GS function. By analyzing the DTI ALPS index of patients with these disorders or diseases, we could diagnose them before they reach an advanced stage, or even, if there are risk factors, diagnose the diseases before clear symptoms have developed or monitor the patients to prevent the development of said disease.

2 Glymphatic system in brain tumors

The glymphatic system and its relationship with brain tumors has recently been the subject of MRI research. Toh et al.[25] studied the formation of peritumoral brain edema (PTBE) and its relationship to the glymphatic system. For meningiomas, they found that the DTI ALPS index was higher in patients in whom PTBE was not present than in those who did have edema and in HCs. Interestingly, they found that the HCs and the patients with tumors and edema had a similar DTI ALPS index. They hypothesized that the tumor and its growth interfere with the balance between the CSF influx and the perivenous efflux of CSF and interstitial fluid, which could be a decisive factor in the formation of peritumoral edema. Next, they studied patients with gliomas. Here, they found that lower-grade gliomas (II/III) had a higher DTI ALPS index than higher-grade ones (IV)[57]. They also observed that the DTI ALPS index was higher in IDH1 mutant tumors than in wild-type tumors. In their research, IDH1 mutation and the volume of the PTBE comprised independent factors associated with the DTI ALPS index. Based on research

pertaining to the expression of AQ4 and its involvement in the formation of PTBE, the authors speculated that changes in AQ4 expression could induce changes in the DTI ALPS index. In that study, however, there were no comparisons with HCs.

Toh and Siow also conducted research on metastases and PTBE[58], calculating the DTI ALPS index as well as other diffusivity characteristics, such as ADC and FA. They found that for cases of larger PTBE the ADC was also higher and the DTI ALPS index lower. They interpreted the higher ADC and lower index as possibly a higher influx of water into the tissue with a lower efflux, potentially contributing to the formation of edema.

The work related to the DTI ALPS index has been so promising that Zhu et al.[59] examined the possibility of using it as a biomarker for grading gliomas. They studied the DTI ALPS index in the brain of patients with glioma, comparing the DTI ALPS index between the hemispheres (one with tumor and one without) as well as in comparison to HCs. They found both a lower DTI ALPS index in the ipsilateral hemisphere of the glioma and a significant decrease in the ALPS index compared to HCs. Then, they analyzed the indices between tumors and found that the index for lower-grade tumors was higher than for the higher-grade ones; they also determined the difference between the IDH1 mutant and wild-type tumor, whereby the former had a higher index. The authors also compared the index to different diffusion metrics and concluded that the DTI ALPS could usefully complement the already available tools to classify the nature of the glioma.

Taking into consideration the available data and the trend of finding a reduced DTI ALPS index in brain tumors, Gao et al.[60] conducted a prospective study. They analyzed patients with different kinds of brain tumors, together with age- and sex-matched HCs, calculated the DTI ALPS index, and investigated the expression of AQ4 in the tissue. According to their results, showing a negative correlation between the DTI ALPS index and the volume of the tumor and a positive correlation between the expression of AQ4 and the volume of PTBE, they hypothesize that the volume and compression due to the tumor could affect glymphatic function and fluid dynamics. This could provide new insight to the pathomechanism underlying PTBE

and offer a new approach to studying the glymphatic system and multiparametric MRI.

2.1 Research question and objectives

The goal of this research was to evaluate the glymphatic system in brain tumors. At the time this research began, other studies on the DTI ALPS index and gliomas[57], meningiomas[25], and edema in brain metastases[58] had already been published.

These studies focused on the side of the brain with the tumor but did not consider comparing the results with those from the contralateral side. Therefore, I aimed to investigate whether there was a significant difference between the brain hemispheres by comparing the DTI ALPS index between the hemispheres with a tumor and without a tumor. I also considered age- and sex-matched HCs and assessed whether there were any relevant differences between hemispheres and with my patient cohort. I also deemed it important to search for relationships between the DTI ALPS index and the origin of the tumor, either primary or secondary, tumor event (first diagnosis or relapse), sex, age, and the ADC of the tumor.

Based on the available literature, I hypothesized that there is an interhemispheric difference in brain tumor patients, in whom a reduced DTI ALPS index would be expected on the tumor side of the brain. Additionally, I expected to detect a difference in the DTI ALPS index between patients and HCs.

3 Material and methods

3.1 Study design

To begin the research, I needed to find a patient cohort. I defined the cohort as patients with an ICD code C71 (malignant brain tumor) or D33 (benign tumor of the brain and other parts of the CNS) in whom an MRI examination was conducted between September 2020 and October 2022. A list of all brain tumor patients that

received an MRI examination was provided by the Department of Organization, Statistics and Revenue Management (Bereich Organisation, Statistiken Dezernat Erlösmanagement) of the University Medical Center Schleswig-Holstein (UKSH). This resulted in a list containing about 800 patients.

Exclusion criteria were: patients under 18, patients who did not receive a DTI and functional MRI examination in the 3-T Siemens Vida MRI System Scanner, or if the images were not free of movement artifacts. To identify statistically significant differences, the study initially included 30 consecutive patients and was approved by the ethics committee of the University of Lübeck (ethical approval 2022-630 and its amendment) (see appendix A).

After retrospectively reviewing the images, it was necessary to expand the exclusion criteria by adding that the area of the periventricular veins should not be affected by the tumor (six patients were excluded). This resulted in a total of 24 patients analyzed in this study (see details in appendix B). The patients were informed about the possible risks associated with an MRI examination as part of clinical routine and they signed a general consent form. As this was a retrospective study, using data from patients obtained as part of clinical routine, study-specific informed consent before the examination was not required. However, HCs provided written informed consent to participate in this study.

Detailed demographic information is shown in Table 2. For comparison, I included healthy participants as controls to match the patients for sex and age (within ± 2 years) and in whom brain MR examination was normal and no history of neurological disorders was present.

3.2 MRI examination

All MRI studies were performed using a 3-T clinical scanner (Magnetom Vida, Siemens Healthineers, Erlangen, Germany) with a 20-channel head coil. The DTI scan was performed using a 2D single-shot echo-planar imaging (EPI) acquisition, with the following parameters: TE/TR = 92/6100 ms; 64 diffusion directions, 2 b-values = 0, and 1000 s/mm^2; field-of-view: 200 x 200 mm^2; matrix size: 100 x 100;

slice thickness: 2 mm, and voxel size: 2 x 2 mm^2. This scan is part of the MR tumor protocol at my clinic and takes 7 min. The ADC map was calculated using the trace image and b = 0. The tumor ADC was calculated over a region-of-interest (ROI) placed at the center of the tumor (area: 5.3 mm^2).

3.3 Image processing

All images were analyzed in MATLAB 2022a (The MathWorks Inc, Natick, Massachusetts, United states) using statistical parameter mapping (SPM) 12 (https://www.fil.ion.ucl.ac.uk/spm) and the diffusion II toolbox (https://sourceforge.net/projects/spmtools/). The diffusion toolbox includes motion correction based on the b = 0 image (with gradient direction correction), and FA, diffusion tensor, and tensor decomposition are calculated. Image quality control was performed by board-certified neuroradiologists.

3.4 Calculation of the DTI ALPS index

The DTI ALPS[24] method uses two ROIs positioned on a single slice at the level of the lateral ventricles. In that region, the direction of the parenchymal vessels is approximately perpendicular to the ventricle wall. Therefore, the perivascular space runs in the same direction: right-left in the patient coordinate system. This concept is explained in Fig. 4. The DTI ALPS index was measured by positioning a ROI of 2 x 2 voxels over one slice (corresponding to an area of 4 x 4 mm^2), as seen in Fig. 5. As a tumor affects brain symmetry, it was not possible to mirror the position of the ROIs in the two hemispheres. Two neuroradiologists with 1 and 10 years of experience in dedicated brain tumor imaging supported in consensus the ROI positioning on the projection and association areas on the ipsi- and contralateral side avoiding PTBE when possible. This was done based on the FA map next to the body of the ventricle. To see the placement of the ROI on the included patients and healthy controls, see appendix C and D respectively. By using the diagonal elements from the diffusion tensor, the DTI ALPS index was calculated as[24]

DTI ALPS index= $\frac{\text{mean (Dxxproj,Dxxass)}}{\text{mean (Dyyproj,Dzzass)}}$, where Dxx, Dyy and Dzz are the diagonal elements of the diffusion tensor.

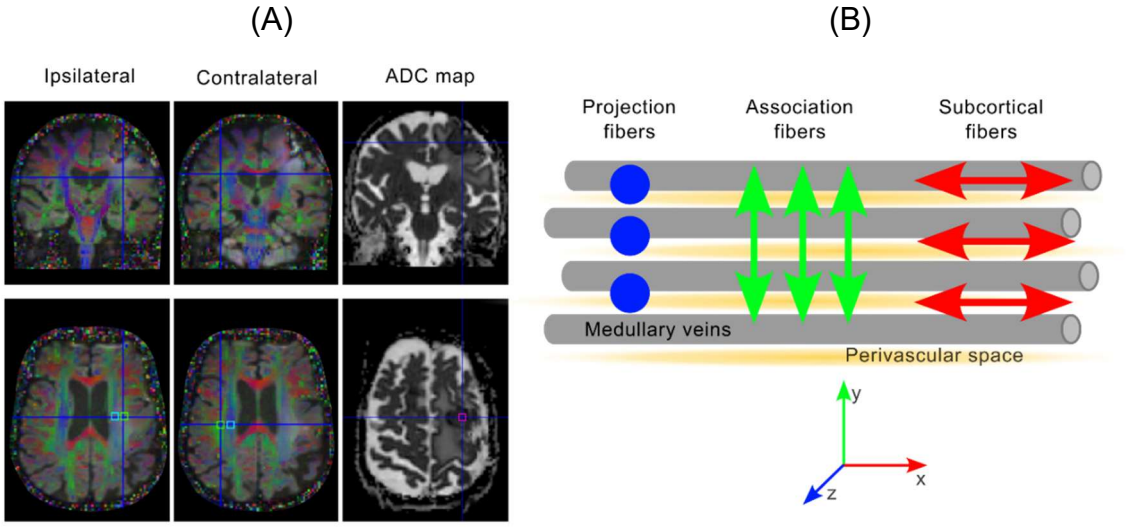

Figure 5 Region-of-interest (ROI) positioning and diffusion tensor imaging along the perivascular spaces (DTI ALPS) concept simplification. (A) Tumor patient (patient no. 3, female, 71 years) with cerebral metastasis (bronchial carcinoma, left frontal). From left to right: fractional anisotropy maps overlaid on a diffusion-trace image and an apparent diffusion coefficient (ADC) map. Squares mark the approximate positions of the ROIs (blue: projection; green: association; and pink: tumor ADC). Note that the ROIs in the ipsilateral side are located inside the peritumoral edema. (B) Concept of DTI ALPS. The projection area (in blue) (i.e., a region dominated by projection fibers in the acquired slice) and association area (in green) contain axonal fibers in feet-head and anterior-posterior directions, respectively. The perivascular space runs perpendicular to these fibers. By using DTI, the diffusivity along the x-axis in the two ROIs (DxxProj and DxxAssoc) would partially represent the diffusivity along the perivascular space in the area next to the lateral ventricles. In the projection area, the dominant fibers are along the z-axis. Therefore, Dxx and Dyy are perpendicular diffusivities while in the association area, the main direction of the fibers is along the y-axis (Dxx and Dzz are the perpendicular diffusivities). The DTI ALPS index is the ratio between the mean of two diffusivities perpendicular to the primary fiber orientation in the projection and association areas (Villacis et al.[23] licensed under Creative Commons Attribution CC BY 4.0.)

3.5 Statistical analysis

MATLAB's statistical toolbox with α = 0.05 significance level was used for statistical analysis. The difference in the DTI ALPS index between the tumor and contralateral side and the HC matching were assessed using the Wilcoxon signed-rank test. DTI ALPS index differences according to age (< 55 vs. > 55 years), sex (male vs. female), and type of tumor (primary vs. secondary) were evaluated using Wilcoxon rank-sum test. In addition, I investigated the relationship between the DTI ALPS index and patient ages and tumor ADC using linear regression.

The normality of the data distribution was assessed by visual analysis of box plots.

The difference in the DTI ALPS index between the tumor and contralateral side and the HC matching were assessed using the Wilcoxon signed-rank test (signrank in Matlab). DTI ALPS index differences according to age (< 55 vs. > 55 years), sex (male vs. female), and type of tumor (primary vs. secondary) were evaluated using the Mann-Whitney U test (ranksum in Matlab). In addition, I investigated the relationship between the DTI ALPS index and patient ages and tumor ADC using linear regression.

4 Results

4.1 Normality definition

To define normality, I have carried out a thorough and balanced analysis of my specific data. My sample size, with 24 patients, is small due to the complexity of the study inclusion and the severely ill patients affected. Statistically, I would have to have at least 30 subjects to be able to test for normality; therefore, non-normally distributed data was assumed. I validated this assumption at a meeting with the Statistical Department of my University by generating a box plot which confirmed that my assumption of non-normality is correct, seen in Fig. 6.

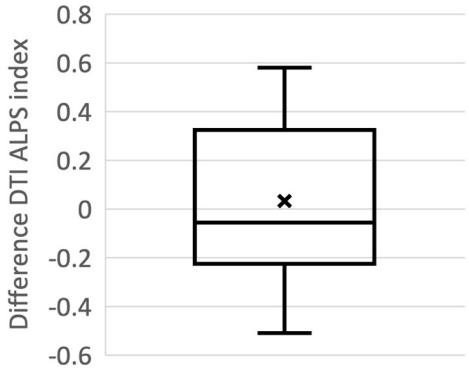

Figure 6 Normality definition with boxplot. This plot shows skewness, with the median not being centered in the box

4.2 Demographics

In this study, 14 male and 10 female patients aged between 24 and 73 years (mean = 56.58 ± 12.71) were included, see Fig. 7. Among these patients, 7 had glioblastomas, 4 diffuse astrocytoma, 3 bronchial carcinoma, 2 oligodendroglioma, 2 multifocal glioblastoma, 2 renal cell carcinoma, 1 mammary cell carcinoma, 1 B-cell lymphoma, 1 convexity meningioma, and 1 with unclear diagnosis, as seen in Fig. 8. Among these patients, 17 had primary tumors (10 patients with local recurrences and 7 with first diagnosis) and 7 cerebral metastases. Five patients did not have PTBE. For more details, see Table 2 in appendix B. Twelve HCs between 24 and 71 years of age (8 males, 4 females; mean age = 52.25 ± 14.20 years) were included. Details are shown in Table 3 in appendix E.

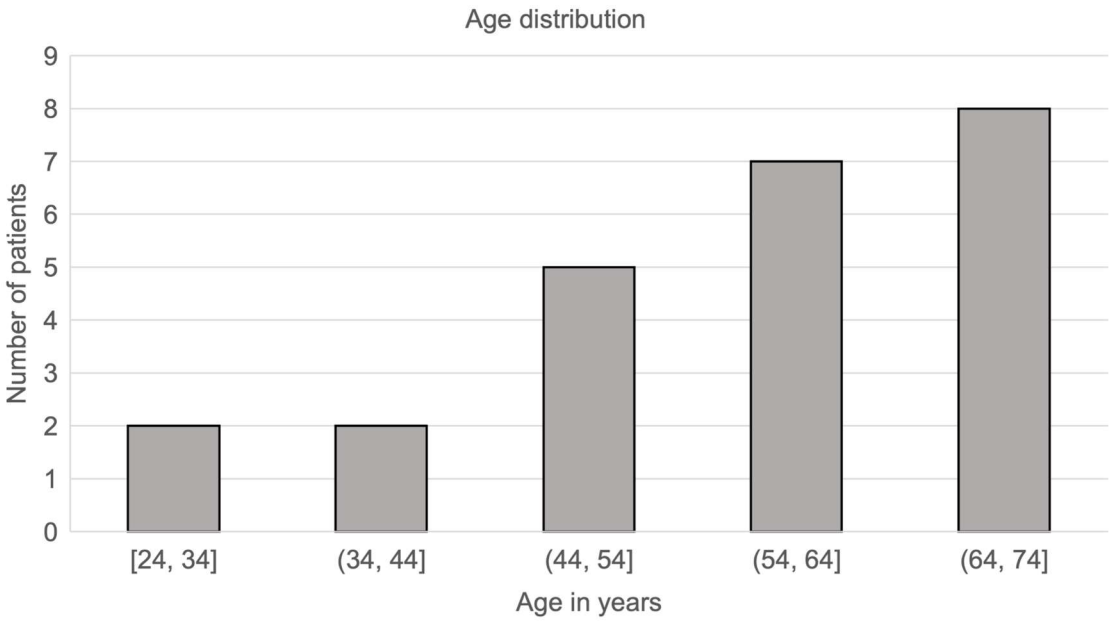

Figure 7 Age distribution of included patients.

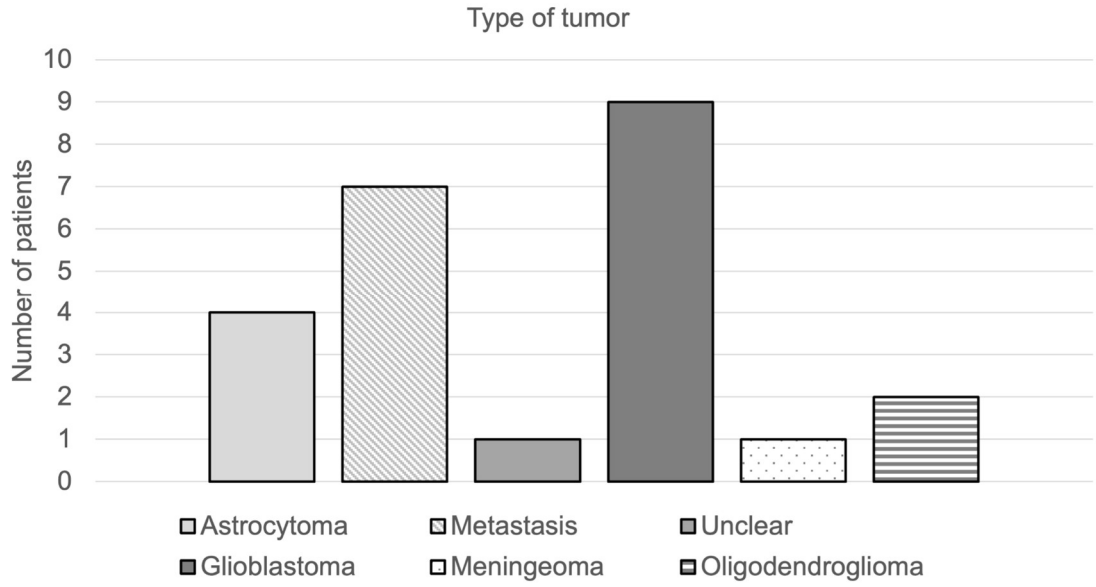

Figure 8 Distribution of tumor entities in included patients

4.3 DTI ALPS index

The DTI ALPS index calculations and comparisons between the ipsi- and contralateral side of the tumors, age, sex, and tumor type are summarized in Table 1. Due to the position of the tumor and the extent of the PTBE, the ipsilateral ROIs were placed in the area of the edema in five patients. However, no significant

differences were observed when the ROI was located inside or outside the PTBE (Mann-Whitney U test, p = 0.065).

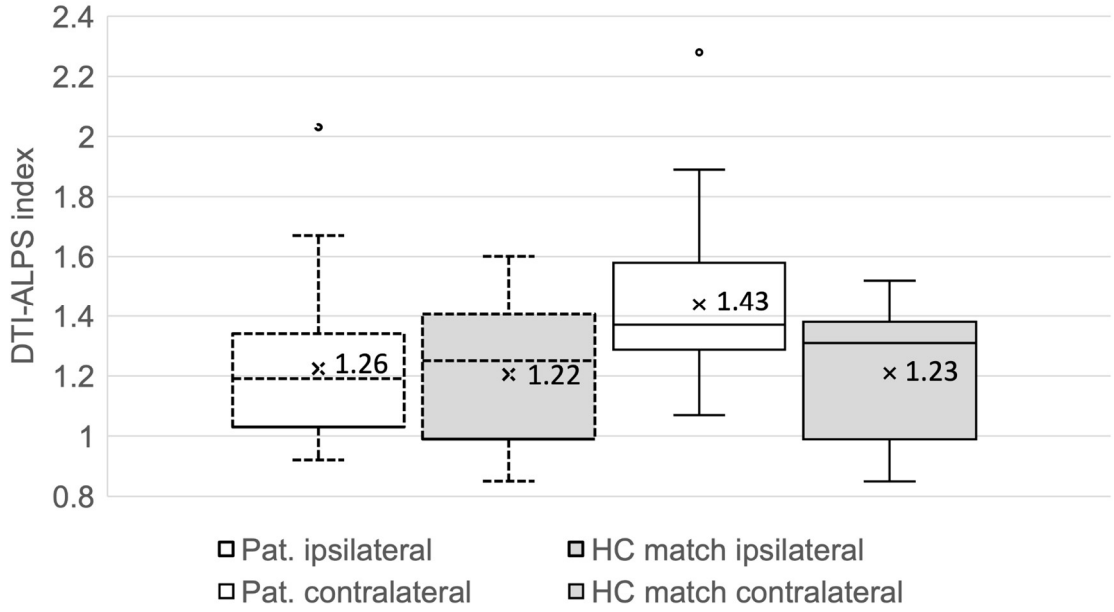

Figure 9 Boxplot showing the difference between the diffusion-tensor imaging across the perivascular spaces (DTI ALPS) index of the tumor side of the brain vs. the contralateral side ($p < 0.05$). For specific values see Table 1.

The most relevant finding of this study is that the DTI ALPS index was significantly lower on the side of the brain with the tumor (DTI ALPS index = 1.26 ± 0.24) than in the contralateral hemisphere (DTI ALPS index = 1.43 ± 0.28) (p = 6.7e-5) (see Fig. 9 and Table 1). When comparing DTI ALPS index in patients and controls, I found no significant difference between the DTI ALPS index between the ipsilateral side of tumor patients and age- and sex-matched controls (HC mean: 1.22 ± 0.22) (p = 0.68). However, there is a significant difference (p = 0.03) when comparing the patients' contralateral side to the HCs (HC mean = 1.23 ± 0.22), where the DTI ALPS index on the patients' contralateral side is larger than that in the HCs. There is no significant difference between the right and left hemispheres in HCs.

Additionally, I did not find any differences in the DTI ALPS index according to age, sex, or type of tumor ($p > 0.05$) (see Table 1). Furthermore, no linear correlation was found between the DTI ALPS index and patient age ($R^2 = 0.0011$, $p = 0.88$ and $R^2 = 0.003$, $p = 0.422$ for the ipsi- and contralateral side, respectively) and tumor

ADC (R^2 = 0.09, p = 0.16) (see Fig. 10 and 11). The average tumor ADC was 1618.42 ± 665.29 mm^2s^{-1}.

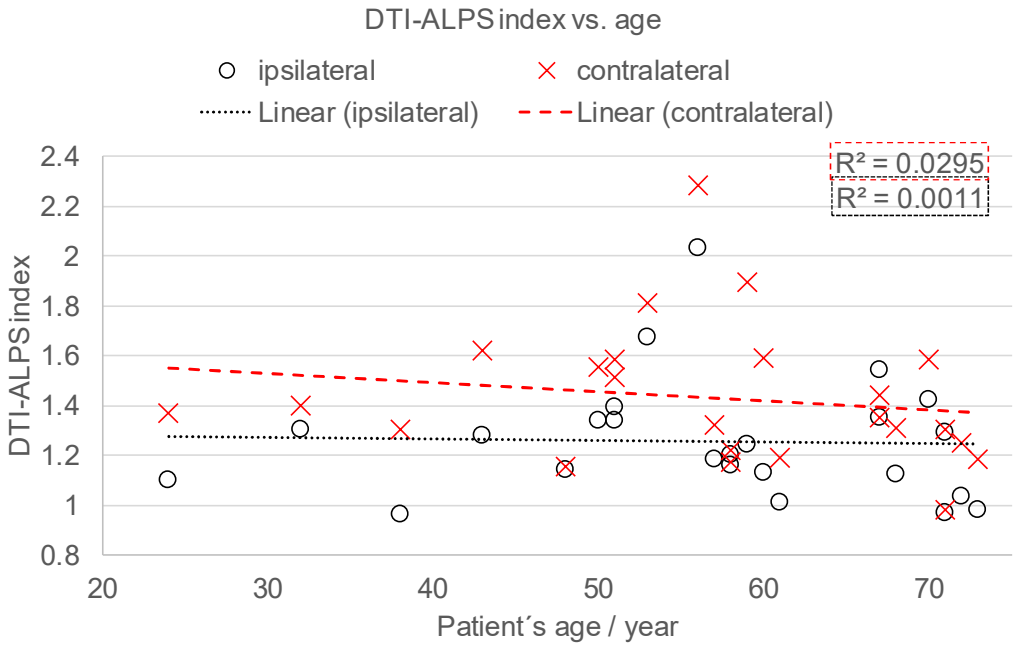

Figure 10 No linear relationship was found between the diffusion-tensor imaging across the perivascular spaces (DTI ALPS) index and patient's age, by hemisphere.

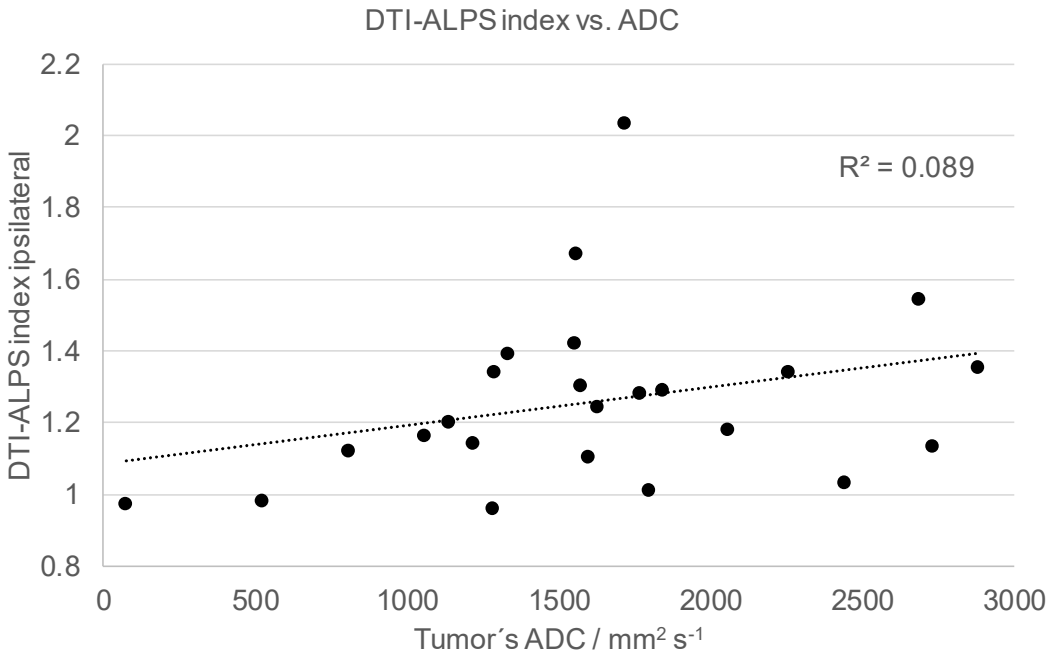

Figure 11 No linear correlation was observed between the diffusion-tensor imaging across the perivascular spaces (DTI ALPS) index and tumor apparent diffusion coefficient (ADC).

Table 1 Comparisons of the diffusion-tensor imaging across the perivascular spaces (DTI ALPS) index according to tumor side, age, sex, and type of tumor. A significant difference is marked with * ($p < 0.05$). Indices are presented as mean ± standard deviation and median (1^{st} quantile, 3^{rd} quantile).

		DTI ALPS index		
Parameter	Participants	mean ± std	median (Q1, Q3)	p
Hemisphere				6.7e-5*
Tumor ipsilateral	24	1.26 ± 0.24	1.22 (1.12, 1.34)	
Tumor contralateral		1.43 ± 0.28	1.36 (1.24, 1.58)	
Age (ipsilateral)				0.51
< 55	9	1.28 ± 0.19	1.30 (1.14, 1.34)	
> 55	15	1.24 ± 0.26	1.18 (1.08, 1.32)	
Age (contralateral)				0.26
< 55		1.48 ± 0.18	1.51 (1.37, 1.58)	
> 55		1.40 ± 0.31	1.31 (1.21, 1.51)	
Sex (ipsilateral)				0.46
Male	14	1.26 ± 0.17	1.29 (1.15, 1.34)	
Female	10	1.25 ± 0.31	1.15 (1.04, 1.32)	
Sex (contralateral)				0.66
Male		1.43 ± 0.18	1.39 (1.30, 1.60)	
Female		1.44 ± 0.37	1.33 (1.18, 1.55)	
Type of tumor (ipsilateral)				0.53
Primary tumor	17	1.28 ± 0.25	1.24 (1.13, 1.34)	
Cerebral metastasis	7	1.20 ± 0.19	1.16 (1.05, 1.32)	
Type of tumor (contralateral)				
Primary tumor		1.49 ± 0.28	1.40 (1.30, 1.58)	0.18
Cerebral metastasis		1.29 ± 0.19	1.31 (1.18, 1.40)	

5 Discussion

Summary of findings

In the present study, I analyzed retrospectively the DTI ALPS index in patients with brain tumors, including both primary brain tumors and cerebral metastases, and compared them to healthy subjects. I compared the DTI ALPS index of the tumor-

affected hemisphere to that of the contralateral side and found statistically significant differences between the hemispheres. In comparison with HCs, I found no difference between the ipsilateral and DTI ALPS index. However, the DTI ALPS index of the contralateral side of the patients was larger than that of the HCs. I suspect there could be a certain degree of compensation to try to maintain the fluid dynamics in the brain.

Furthermore, I did not see a significant difference between the DTI ALPS index and the type of tumor (primary or brain metastasis). Moreover, I did not find significant group differences according to age, sex, or type of tumor. Nor did I find a linear correlation between DTI ALPS index and age and tumor ADC.

DTI ALPS index and brain tumors

To my knowledge, at the time this research was conducted, only three publications so far had used the DTI ALPS method to assess GS function in patients suffering from brain tumors[25,57,58]. However, only the study in meningioma[25] considered the tumor's contralateral side and included HCs.

The DTI ALPS index in brain tumors has been evaluated by Toh et al.[25,57,58]. First, they analyzed the formation of PTBE in meningiomas[25]. In that study, they compared the DTI ALPS index in patients with meningiomas with and without PTBE and HC. They found that the DTI ALPS index was larger in patients without PTBE than in both healthy subjects and patients with edema. There was no difference between the patients with edema and the HC. These findings partially agree with my results, where there is no significant difference between the ipsilateral side and the matched HCs and that the DTI ALPS index was larger in tumor patients than HCs. However, contrary to my findings, they did not find a significant difference between the ipsi- and contralateral hemispheres in meningioma patients, without further discussion. I speculate that for this reason, they did not investigate the DTI ALPS index in the tumor's nonaffected contralateral side in further research. I could hypothesize that intra- and extra-axial tumors may affect the GS function using different mechanisms. However, I cannot draw definitive conclusions and more research is needed here[25].

Secondly, Toh and Siow[57] investigated GS function in patients with gliomas using DTI ALPS in the hemisphere of the tumor. They compared the DTI ALPS index in patients with different stages of glioma, the type of IDH1, and the sex of the patients. They found a significant difference in the DTI ALPS index between patients with a lower-grade glioma and those with a higher-grade glioma (II/III grade vs. IV grade glioma). Additionally, the index for the mutant IDH1 was higher than that for the wild-type mutation. However, the authors did not include HCs in this research.

Lastly, the authors studied perivascular edema in brain metastases[58]. They found that high ADC tumor values and low DTI ALPS index were related to large edema volumes. This suggests that high volumes of edema may be related to intratumoral water diffusivity, disturbing glymphatic function. I did not find a significant relationship between a tumor's ADC and the DTI ALPS index. However, the main focus of Toh et al.[58] was PTBE and, therefore, I cannot directly compare my conclusions.

In contrast to Toh et al.[58], I did not find a linear correlation between the tumor ADC and DTI ALPS index. However, due to my small sample size, further studies are needed to evaluate these parameters. These contradicting results could be due to differences in calculating the ADC in the tumor. I selected a small area in the middle of the tumor, while they calculated the ADC by taking an average of all slices where the tumor was present. However, I did not investigate PTBE and thus cannot directly compare this parameter.

In addition, the DTI ALPS index of the contralateral side of the patients was larger than the one from HCs in my work, contradicting the study of Toh et al. on meningiomas[25].

Previous publications have not observed any significant differences between patients and controls, such as in Parkinson's disease[61], focal epilepsy[51], and migraine[62]. However, to my knowledge, no publication has reported a higher index in patients than in healthy subjects. One could hypothesize that the diffusion along perivascular spaces in the contralateral side is abnormally enlarged in patients in an attempt to compensate for the increased amount of brain waste products due to the

increased metabolic activity in the tumor, tissue compression, and general neuroinflammation. However, no definitive conclusions can be made yet and further research is required.

Moreover, one needs to consider that Toh et al.[25] mainly studied PTBE in extra-axial tumors and its influence on DTI ALPS index, and I did not distinguish between patients with and without PTBE.

DTI ALPS index interhemispheric differences

I would argue that the contralateral hemisphere should be analyzed in particular when considering gliomas as it must increasingly be assumed that higher-grade gliomas do not only show abnormalities in pathologically contrast-enhancing lesions on MRI[63] but also in far more extensive anatomical areas. Cerebral glioma must increasingly be evaluated as a disease of larger parts of the brain, if not of the entire brain. Therefore, determining the DTI ALPS index in the contralateral hemisphere, too, is significant.

Additionally, the study of both hemispheres is interesting because in patients with epilepsy[51,53,64,65], for example, the DTI ALPS index on the ipsilateral side was lower than on the contralateral side, suggesting reduced glymphatic system function in the hemisphere ipsilateral to the epileptogenic foci. Other examples include ischemic[66,67] and hemorrhagic[68] stroke and traumatic brain injury[69], where the DTI ALPS index on the ipsilateral side was reduced in comparison with the contralateral hemisphere. Furthermore, considering that results have been inconsistent as to whether the differences between dominant and nondominant brain hemispheres are significant in normal subjects, the lateralization of the DTI ALPS index in HCs and patients requires further study[70].

I also analyzed GS function in both primary and secondary tumors in the brain using DTI ALPS in the ipsi- and contralateral sides of the brain and compared the results with those of HCs. I hypothesized that GS function would be lower on the side of the brain with the tumor than on the contralateral side. I also evaluated

differences in DTI ALPS index between sex, age, and tumor histology (primary vs. brain metastasis).

In addition, as the peritumoral edema of cerebral metastases has been reported as positively correlating with tumor ADC and inversely with the DTI ALPS index[58] I investigated whether there is a correlation between tumor ADC and DTI ALPS in my cohort. In addition, a dependence between DTI ALPS index and age has been observed in healthy subjects[71]. Therefore, in this work, I wanted to investigate whether there is a correlation between age and DTI ALPS index in brain tumor patients.

As expected, I found that the DTI ALPS index in the ipsilateral hemisphere was lower than that on the contralateral side, suggesting impaired glymphatic function on the side of the brain with the tumor. However, due to different tumor locations, the anatomy of the brain and periventricular veins may be altered and measuring the diffusivity along the perivascular spaces in the ipsilateral side may not be totally free from undesired influences due to anatomical displacements. Therefore, I excluded patients in whom the area of the periventricular veins was affected by the position of the tumor, as seen in appendix F.

DTI ALPS and demographic parameters

In my cohort, I did not find significant gender differences regarding the DTI ALPS index results. This is consistent with the findings of other DTI ALPS tumor-related studies[25,57,58]. Previous studies investigating the DTI ALPS index difference between males and females reached the same conclusion[61,66,69,72–77] that there is no significant difference between sexes. However, contradictory results have been reported by Hsiao et al.[78] and Zhang et al.[79], where the DTI ALPS index in women was larger than in men. Thus, further investigation into different illnesses with a larger sample size might still be required to determine whether sex differences play a role.

Previous studies found a negative correlation between age and DTI ALPS index[20,46,51–53,78,80,81]. This is a common finding in healthy volunteers and in

neurodegenerative diseases such as Parkinson's and Alzheimer's disease. However, in cases of brain tumors[25,57,58], REM sleep disorder[82], neuromyelitis optica[83], renal disease[84,85], global amnesia[86], and migraine[62] no significant correlation has been found between DTI ALPS and age. Nor did I find any correlation between patients' age and DTI ALPS index in my research.

The relationship between age and DTI ALPS index should be further studied to determine which factors might be involved in the changes in diffusion along perivascular spaces under other clinical conditions.

Possible differences between intra- and extra-axial tumors

Additionally, intra-axial tumors can directly disrupt the microstructure of the brain and directly affect water diffusion in the brain due to cellular growth or tumor cell infiltration, for example. On the other hand, extra-axial tumors, due to mass effect, can compress and exert pressure on adjacent structures but typically do not directly infiltrate brain tissue. This could suggest the existence of different brain waste clearance mechanisms. Furthermore, as the DTI ALPS index is measured in the deep white matter, it is no wonder that the ADCs in the tumor-affected hemisphere will differ from the contralateral side in the case of intra-axial tumors. However, both tumor types could compress the brain, or the extra-axial tumors could infiltrate the perivascular spaces, like the periventricular veins. Therefore, extra-axial tumor infiltration into brain tissue might have different effects on deep white matter than tumors which don´t infiltrate it, a topic that needs to be investigated separately.

5.1 Clinical relevance

By studying the glymphatic system and calculating the DTI ALPS index we are able to quantify diffusion in the perivascular space in the area of the periventricular veins. This will facilitate a better understanding of fluid dynamics and pathophysiology in the CNS, specifically of the CSF and interstitial fluid (ISF) in the brain parenchyma. Once our understanding of the DTI ALPS index and its applications has been refined, this knowledge can potentially influence the way we diagnose, treat, and prevent neurological diseases and complications.

The DTI ALPS index could become a biomarker and screening tool for many diseases, including brain tumors in patients with a family history of cancer, where a reduced index could serve as a tool for early detection of tumoral development. This could have a huge impact on treatment possibilities and interventions. For example, in the case of PTBE, a relationship between the DTI ALPS index and its formation has been observed. By including imaging and calculating the DTI ALPS index patients prone to developing PTBE or more severe edema could be identified and drugs administered at an early stage could influence disease development. We could also establish strategies for patients with a low DTI ALPS index in whom waste clearance of the brain is suspected to be reduced so as to stimulate the waste clearance system to reduce or prevent the appearance of edema, high intracranial pressure, and the development and severity of neurological symptoms. This could also apply in postoperative care, where patients with a lower DTI ALPS index on preoperative images would receive more intensive rehabilitation to prevent a decline in neurological functions. My research showed an impaired glymphatic system in the ipsilateral side in brain tumors. Therefore, it seems conceivable that the DTI ALPS index could be used as a biomarker for disease progression, which could prompt early interventions, contributing to reducing complications and even greater treatment success. More research is needed to explore these possibilities.

Additionally, an impaired glymphatic system could mean that drugs passing the BBB would take longer to reach the target area or remain longer in the area, causing complications in the treatment of diseases that already present significant challenges. In patients in whom impairment of the glymphatic system does not play a relevant role, new treatments can be developed to take advantage of the function of the glymphatic system to distribute medication. In the case of impairment, targeted treatments may bypass the area where the glymphatic system is affected, potentially being more effective.

To my knowledge, only little research has been conducted on radiotherapy and its impact on glymphatic function. Thus, potential optimization of treatments would be expected once the mechanisms of the glymphatic system and the DTI ALPS index are better understood.

It has been hypothesized that an impairment of the glymphatic system and the accumulation of waste molecules could be the cause of neurodegeneration and linked to many diseases. With a better understanding of the DTI ALPS index, it could potentially serve as a biomarker of these diseases and, with careful interpretation, potentially reveal the degree of neurodegeneration to be expected and possible future symptoms.

5.2 Limitations and future work

Here, I compare the DTI ALPS index of the brain tumor hemisphere with the contralateral side as well as differences between tumor type, age, and sex. Additionally, I included HCs to compare the DTI ALPS indexes. Nonetheless, there are several limitations that need to be addressed:

Sample size

The sample size of this single-center, retrospective, consecutive study is small. Further studies should consist of more tumor patients and age- and sex-matched HCs. Additionally, the study lacks data about the clinical course of the patients; thus, I cannot correlate GS dysfunction with subsequent, distinct psychiatric or neurological deficits. Further studies should therefore correlate the DTI ALPS index with corresponding neuropsychological parameters.

ROI planning

The correct planning of the ROIs can be difficult and may require practice. In this study, a senior and junior neuroradiologist supported the positioning of the ROIs in consensus. Additionally, I planned the ROIs using only the FA image, as susceptibility-weighted images are not part of clinical routine at my institution. This forced me to assume that the paraventricular veins are parallel to each other and perpendicular to the lateral ventricle, but as I did not have images of the blood vessels, I cannot guarantee that there no anatomical variations were present in my cohort. Also, the manual positioning of the ROIs using SPM 12 was not user-friendly. Under certain rotations in appeared to be uneven (see appendix G). Further studies should include susceptibility-weighted images for positioning of the ROIs in order to

determine whether the course of the periventricular and peritumoral blood vessels has an effect here.

Issues inherent to the DTI ALPS method

The DTI ALPS method estimates diffusivity along the perivascular space in a small ROI parallel to the medullary veins, which extrapolates that the whole-brain glymphatic function could be derived from this small area within deep white matter, while amyloid β and tau proteins are produced and accumulate in the brain cortex[87]. Furthermore, the DTI ALPS index does not solely represent diffusion in the perivascular space, but also other processes, such as axonal degeneration[88]; and therefore, cannot be directly linked to GS function. In addition, due to different tumor locations, the anatomy of the brain and periventricular veins may be altered and measuring the diffusivity along the perivascular spaces in the ipsilateral side may not be totally free from undesired influences due to anatomical displacements, also potentially not reflecting brain waste clearance directly. Hence, changes in the DTI ALPS index should be interpreted with caution[38,88,89].

6 Conclusion

The DTI ALPS appears to be an excellent noninvasive technique to evaluate GS function. The lower DTI ALPS index of the ipsilateral hemisphere might suggest that GS function is impaired in patients with brain tumors. Although the DTI ALPS index was larger on the contralateral side, one should not consider this value as a HC. As brain tumors often affect larger areas, if not the whole brain, one could expect a general GS disruption. Further studies are needed to investigate the GS and its relationship between the DTI ALPS index and different histological brain tumor entities. The DTI ALPS index might be suitable as a biomarker for GS status and function in patients with tumors in the brain.

I was also aware that certain anatomical complications could arise when tumors are present. Due to their growth, the possibility of altered anatomy remained. Additionally, as I measured the DTI ALPS index in my ROIs, a direct extrapolation

in an already diseased brain to the glymphatic function of the whole brain could be considered an assumption. I am aware that further studies are necessary to cement my theory and research but am confident that my results can contribute to a better understanding of the glymphatic system and of changes that might appear at the molecular level in a brain harboring a tumor.

As the factors influencing the DTI ALPS index are still unknown, interpretation of changes in this index should not be directly linked to GS function. Caution in drawing conclusions is therefore advised.

7 Summary

Research question To investigate glymphatic system function in patients with brain tumors, including both primary and secondary tumors, using diffusion-tensor imaging along perivascular spaces (DTI ALPS).

Methods I retrospectively analyzed magnetic resonance DTI of 24 patients with unilateral brain tumors and compared them with age- and sex-matched controls. I compared the DTI ALPS index of the ipsi- and contralateral brain hemispheres. The region-of-interest was placed in the periventricular vessels adjacent to the lateral ventricles. Differences between sex, age, and type of tumor (primary or brain metastasis) were evaluated. Correlations between DTI ALPS index and age and the tumor's apparent diffusion coefficient (ADC) were also investigated.

Results The DTI ALPS index was significantly lower ($p < 0.05$) in the tumor-affected hemisphere (mean = 1.26 ± 0.24) than on the contralateral side (mean = 1.43 ± 0.28). A comparison with healthy controls revealed no significant difference on the matched ipsilateral side. However, the DTI ALPS index of contralateral side of the patients was larger than that for healthy controls. Additionally, no statistically significant differences were found when analyzing the DTI ALPS index vs. age, sex, and tumor entity. Additionally, I did not find a correlation between the DTI ALPS index and patient age or tumor ADC.

Conclusion and discussion The decreased DTI ALPS index in the tumor-affected hemisphere may be related to impaired glymphatic system function. However, cancer is often a systemic disease; thus, the DTI ALPS index from the contralateral brain hemisphere may not generally be considered as a normal control. Yet, DTI ALPS appears to be a suitable technique for evaluating the glymphatic system noninvasively.

8 References

1. Clarke DD, Sokoloff L. Regulation of cerebral metabolic rate. In: Siegel GJ, Agranoff BW, Albers RW, et al., Editors. Basic Neurochemistry: Molecular, Cellular and Medical Aspects. 6th Edition. Philadelphia: Lippincott-Raven; 1999. Available from: https://www.ncbi.nlm.nih.gov/books/NBK28194/.

2. Zhang ET, Inman C B, Weller, R O. Interrelationships of the pia mater and the perivascular (Virchow-Robin) spaces in the human cerebrum. J Anat. 1990;170:111-123.

3. Albargothy NJ, Johnston DA, MacGregor-Sharp M, et al. Convective influx/glymphatic system: tracers injected into the CSF enter and leave the brain along separate periarterial basement membrane pathways. Acta Neuropathol. 2018;136(1):139-152. doi:10.1007/s00401-018-1862-7

4. Aspelund A, Antila S, Proulx ST, et al. A dural lymphatic vascular system that drains brain interstitial fluid and macromolecules. J Exp Med. 2015;212(7):991-999. doi:10.1084/jem.20142290

5. Zlokovic BV. Neurovascular pathways to neurodegeneration in Alzheimer's disease and other disorders. Nat Rev Neurosci. 2011;12(12):723-738. doi:10.1038/nrn3114

6. Bohr T, Hjorth PG, Holst SC, et al. The glymphatic system: Current understanding and modeling. iScience. 2022;25(9):104987. doi:10.1016/j.isci.2022.104987

7. Iliff JJ, Wang M, Liao Y, et al. A Paravascular pathway facilitates CSF flow through the brain parenchyma and the clearance of interstitial solutes, including amyloid β. Sci Transl Med. 2012;4(147). doi:10.1126/scitranslmed.3003748

8. Jessen NA, Munk ASF, Lundgaard I, Nedergaard M. The glymphatic system: A beginner's guide. Neurochem Res. 2015;40(12):2583-2599. doi:10.1007/s11064-015-1581-6

9. Antoine Louveau, Igor Smirnov, Timothy J. Keyes, Jacob D. Eccles, Sherin J. Rouhani, J. David Peske, Noel C. Derecki, David Castle, James W. Mandell, Kevin S. Lee, Tajie H. Harris, Jonathan Kipnis. Structural and functional features of central nervous system lymphatic vessels. Nature. 2015;523:337-341. doi:https://doi.org/10.1038/nature14432

10. Absinta M, Ha SK, Nair G, et al. Human and nonhuman primate meninges harbor lymphatic vessels that can be visualized noninvasively by MRI. eLife. 2017;6:e29738. doi:10.7554/eLife.29738

11. Naganawa S, Taoka T. The glymphatic system: A review of the challenges in visualizing its structure and function with MR imaging. Magn Reson Med Sci. 2022;21(1):182-194. doi:10.2463/mrms.rev.2020-0122

12. Eide PK, Vatnehol SAS, Emblem KE, Ringstad G. Magnetic resonance imaging provides evidence of glymphatic drainage from human brain to cervical lymph nodes. Sci Rep. 2018;8(1):7194. doi:10.1038/s41598-018-25666-4

13. Ren X, Liu S, Lian C, et al. Dysfunction of the glymphatic system as a potential mechanism of perioperative neurocognitive disorders. Front Aging Neurosci. 2021;13:659457. doi:10.3389/fnagi.2021.659457

14. Iliff JJ, Wang M, Zeppenfeld DM, et al. Cerebral arterial pulsation drives paravascular CSF–interstitial fluid exchange in the murine brain. J Neurosci. 2013;33(46):18190-18199. doi:10.1523/JNEUROSCI.1592-13.2013

15. Yamada S, Miyazaki M, Yamashita Y, et al. Influence of respiration on cerebrospinal fluid movement using magnetic resonance spin labeling. Fluids Barriers CNS. 2013;10(1):36. doi:10.1186/2045-8118-10-36

16. Lee H, Xie L, Yu M, et al. The effect of body posture on brain glymphatic transport. J Neurosci. 2015;35(31):11034-11044. doi:10.1523/JNEUROSCI.1625-15.2015

17. Weller RO, Subash M, Preston SD, Mazanti I, Carare RO. Perivascular drainage of amyloid-beta peptides from the brain and its failure in cerebral amyloid

angiopathy and Alzheimer's disease. Brain Pathol. 2007;18(2):253-266. doi:10.1111/j.1750-3639.2008.00133.x

18. Tan C, Wang X, Wang Y, et al. The pathogenesis based on the glymphatic system, diagnosis, and treatment of idiopathic normal pressure hydrocephalus. Clin Interv Aging. 2021; Volume 16:139-153. doi:10.2147/CIA.S290709

19. Yokota H, Vijayasarathi A, Cekic M, et al. Diagnostic performance of glymphatic system evaluation using diffusion tensor imaging in idiopathic normal pressure hydrocephalus and mimickers. Curr Gerontol Geriatr Res. 2019;2019:1-10. doi:10.1155/2019/5675014

20. Xin Cai, Chen Z, He C, et al. Diffusion along perivascular spaces provides evidence interlinking compromised glymphatic function with aging in Parkinson's disease. CNS Neurosci Ther. 2023;29(1):111-121. doi:10.1111/cns.13984

21. Iliff JJ, Lee H, Yu M, et al. Brain-wide pathway for waste clearance captured by contrast-enhanced MRI. J Clin Invest. 2013;123(3):1299-1309. doi:10.1172/JCI67677

22. Patel M, Atyani A, Salameh JP, McInnes M, Chakraborty S. Safety of intrathecal administration of gadolinium-based contrast agents: A systematic review and meta-analysis. Radiology. 2020;297(1):75-83. doi:10.1148/radiol.2020191373

23. Villacis G, Schmidt A, Rudolf JC, et al. Evaluating the glymphatic system via magnetic resonance diffusion tensor imaging along the perivascular spaces in brain tumor patients. Jpn J Radiol. 2024;42(10):1146-1156. doi:10.1007/s11604-024-01602-7

24. Taoka T, Masutani Y, Kawai H, et al. Evaluation of glymphatic system activity with the diffusion MR technique: diffusion tensor image analysis along the perivascular space (DTI-ALPS) in Alzheimer's disease cases. Jpn J Radiol. 2017;35(4):172-178. doi:10.1007/s11604-017-0617-z

25. Toh CH, Siow TY, Castillo M. Peritumoral brain edema in meningiomas may be related to glymphatic dysfunction. Front Neurosci. 2021;15:674898. doi:10.3389/fnins.2021.674898

26. Garzorz-Stark, Natalie. Basics neuronatomie. 2nd Edition. New York, NY, USA. Elsevier; 2018.

27. Deuschl G, Beghi E, Fazekas F, et al. The burden of neurological diseases in Europe: an analysis for the Global Burden of Disease Study 2017. Lancet Public Health. 2020;5(10):e551-e567. doi:10.1016/S2468-2667(20)30190-0

28. Bertolini F, Spallanzani A, Fontana A, Depenni R, Luppi G. Brain metastases: an overview. CNS Oncol. 2015;4(1):37-46. doi:10.2217/cns.14.51

29. Pinto, Marija. Basics Neurologie. 7. Auflage. Urban & Fischer in Elsevier; 2023.

30. Osborn AG, Louis DN, Poussaint TY, Linscott LL, Salzman KL. The 2021 world health organization classification of tumors of the central nervous system: What neuroradiologists need to know. AJNR Am J Neuroradiol. 2022;43(7):928-937. doi:10.3174/ajnr.A7462

31. Louis DN, Perry A, Wesseling P, et al. The 2021 WHO classification of tumors of the central nervous system: A summary. Neuro Oncol. 2021;23(8):1231-1251. doi:10.1093/neuonc/noab106

32. Tan IL, Perez AR, Lew RJ, et al. Targeting the non-coding genome and temozolomide signature enables CRISPR-mediated glioma oncolysis. Cell Rep. 2023;42(11):113339. doi:10.1016/j.celrep.2023.113339

33. Blink, Evert J. Basic MRI Physics. Published online 2010. Available from: https://faculty.washington.edu/seattle/physics541/%202010-reading/mri-physics-uk.pdf

34. Corradini S, Alongi F, Andratschke N, et al. MR-guidance in clinical reality: Current treatment challenges and future perspectives. Radiat Oncol. 2019;14(1):92. doi:10.1186/s13014-019-1308-y

35. Le Bihan D, Mangin J, Poupon C, et al. Diffusion tensor imaging: Concepts and applications. J Magn Reson Imaging. 2001;13(4):534-546.doi:10.1002/jmri.1076

36. Kono, K., Inoue, K., Nakayama, K.,Shakudo, M., Morino, M., Ohata, K., Wakasa, K., Yamada, R. The role of diffusion-weighted imaging in patients with brain tumors. AJNR Am J Neuroradiol. 2018;6(2). doi:10.18535/jmscr/v6i2.95

37. Basser, P., Mattiello, J., LeBihan, D. Estimation of the effective self-diffusion tensor from the NMR spin echo. J Magn Reson B. 1994;(103):247-254. doi: 10.1006/jmrb.1994.1037.

38. Taoka T, Ito R, Nakamichi R, Nakane T, Kawai H, Naganawa S. Diffusion tensor image analysis along the perivascular apace (DTI-ALPS): Revisiting the meaning and significance of the method. Magn Reson Med Sci. 2024< 23(3):268-290. doi:10.2463/mrms.rev.2023-0175

39. Si X, Guo T, Wang Z, et al. Neuroimaging evidence of glymphatic system dysfunction in possible REM sleep behavior disorder and Parkinson's disease. NPJ Parkinsons Dis. 2022;8(1):54. doi:10.1038/s41531-022-00316-9

40. Ma X, Li S, Li C, et al. Diffusion tensor imaging along the perivascular space index in different stages of Parkinson's disease. Front Aging Neurosci. 2021;13:773951. doi:10.3389/fnagi.2021.773951

41. McKnight CD, Trujillo P, Lopez AM, et al. Diffusion along perivascular spaces reveals evidence supportive of glymphatic function impairment in Parkinson disease. Parkinsonism Relat Disord. 2021;89:98-104. doi:10.1016/j.parkreldis.2021.06.004

42. Ruan X, Huang X, Li Y, Li E, Li M, Wei X. Diffusion tensor imaging analysis along the perivascular space index in primary Parkinson's disease patients with and without freezing of gait. Neuroscience. 2022;506:51-57. doi:10.1016/j.neuroscience.2022.10.013

43. Chen HL, Chen PC, Lu CH, et al. Associations among cognitive functions, plasma DNA, and diffusion tensor image along the perivascular space (DTI-

ALPS) in patients with Parkinson's disease. Oxid Med Cell Longev. 2021;2021:1-10. doi:10.1155/2021/4034509

44. Bae YJ, Kim JM, Choi BS, et al. Glymphatic function assessment in Parkinson's disease using diffusion tensor image analysis along the perivascular space. Parkinsonism Relat Disord. 2023;114:105767. doi: 10.1016/j.parkreldis.2023.105767

45. Sundaram S, Hughes RL, Peterson E, et al. Establishing a framework for neuropathological correlates and glymphatic system functioning in Parkinson's disease. Neurosci Biobehav Rev. 2019;103:305-315. doi: 10.1016/j.neubiorev.2019.05.016

46. Hsu J, Wei Y, Toh CH, et al. Magnetic resonance images implicate that glymphatic alterations mediate cognitive dysfunction in Alzheimer disease. Ann Neurol. 2023;93(1):164-174. doi:10.1002/ana.26516

47. Steward CE, Venkatraman VK, Lui E, et al. Assessment of the DTI-ALPS parameter along the perivascular space in older adults at risk of dementia. J Neuroimaging. 2021;31(3):569-578. doi:10.1111/jon.12837

48. Zhang X, Wang Y, Jiao B, et al. Glymphatic system impairment in Alzheimer's disease: associations with perivascular space volume and cognitive function. Eur Radiol. 2023;34(2):1314-1323. doi:10.1007/s00330-023-10122-3

49. Toh CH, Siow TY. Glymphatic dysfunction in patients with ischemic stroke. Front Aging Neurosci. 2021;13:756249. doi:10.3389/fnagi.2021.756249

50. Lee HJ, Lee DA, Shin KJ, Park KM. Glymphatic system dysfunction in patients with juvenile myoclonic epilepsy. J Neurol. 2022;269(4):2133-2139. doi:10.1007/s00415-021-10799-w

51. Lee DA, Park BS, Ko J, et al. Glymphatic system function in patients with newly diagnosed focal epilepsy. Brain Behav. 2022;12(3). doi:10.1002/brb3.2504

52. Lee DA, Lee J, Park KM. Glymphatic system impairment in patients with status epilepticus. Neuroradiology. 2022;64(12):2335-2342. doi:10.1007/s00234-022-03018-4

53. Lee DA, Park BS, Ko J, et al. Glymphatic system dysfunction in temporal lobe epilepsy patients with hippocampal sclerosis. Epilepsia Open. 2022;7(2):306-314. doi:10.1002/epi4.12594

54. Ringstad G, Vatnehol SAS, Eide PK. Glymphatic MRI in idiopathic normal pressure hydrocephalus. Brain. 2017;140(10):2691-2705. doi:10.1093/brain/awx191

55. Eide PK, Ringstad G. Delayed clearance of cerebrospinal fluid tracer from entorhinal cortex in idiopathic normal pressure hydrocephalus: A glymphatic magnetic resonance imaging study. J Cereb Blood Flow Metab. 2019;39(7):1355-1368. doi:10.1177/0271678X18760974

56. Bae YJ, Kim JM, Choi BS, et al. Altered brain glymphatic flow at diffusion-tensor MRI in rapid eye movement sleep behavior disorder. Radiology. 2023;307(5):e221848. doi:10.1148/radiol.221848

57. Toh CH, Siow TY. Factors associated with dysfunction of glymphatic system in patients with glioma. Front Oncol. 2021;11:744318. doi:10.3389/fonc.2021.744318

58. Toh CH, Siow TY, Castillo M. Peritumoral brain edema in metastases may be related to glymphatic dysfunction. Front Oncol. 2021;11:725354. doi:10.3389/fonc.2021.725354

59. Zhu H, Xie Y, Li L, et al. Diffusion along the perivascular space as a potential biomarker for glioma grading and isocitrate dehydrogenase 1 mutation status prediction. Quant Imaging Med Surg. 2023;13(12):8259-8273. doi:10.21037/qims-23-541

60. Gao M, Liu Z, Zang H, et al. A histopathologic correlation study evaluating glymphatic function in brain tumors by multiparametric MRI. Clin Cancer Res.2024;30(21):4876-4886. doi:10.1158/1078-0432.CCR-24-0150

61. Ma X, Li S, Li C, et al. Diffusion tensor imaging along the perivascular space index in different stages of parkinson's disease. Front Aging Neurosci. 2021;13:773951. doi:10.3389/fnagi.2021.773951

62. Lee DA, Lee H, Park KM. Normal glymphatic system function in patients with migraine: A pilot study. Headache. 2022;62(6):718-725. doi:10.1111/head.14320

63. Kessler AT, Bhatt AA. Brain tumour post-treatment imaging and treatment-related complications. Insights Imaging. 2018;9(6):1057-1075. doi:10.1007/s13244-018-0661-y

64. Zhao X, Zhou Y, Li Y, et al. The asymmetry of glymphatic system dysfunction in patients with temporal lobe epilepsy: A DTI-ALPS study. J Neuroradiol. 2023;50(6):562-567. doi:10.1016/j.neurad.2023.05.009

65. Zhang C, Xu K, Zhang H, et al. Recovery of glymphatic system function in patients with temporal lobe epilepsy after surgery. Eur Radiol. 2023;33(9):6116-6123. doi:10.1007/s00330-023-09588-y

66. Toh CH, Siow TY. Glymphatic dysfunction in patients with ischemic stroke. Front Aging Neurosci. 2021;13:756249. doi:10.3389/fnagi.2021.756249

67. Qin Y, Li X, Qiao Y, et al. DTI-ALPS: An MR biomarker for motor dysfunction in patients with subacute ischemic stroke. Front Neurosci. 2023;17:1132393. doi:10.3389/fnins.2023.1132393

68. Zhang C, Sha J, Cai L, et al. Evaluation of the glymphatic system using the DTI-ALPS index in patients with spontaneous intracerebral haemorrhage. Oxid Med Cell Longev. 2022;2022:2694316. doi:10.1155/2022/2694316

69. Park JH, Bae YJ, Kim JS, et al. Glymphatic system evaluation using diffusion tensor imaging in patients with traumatic brain injury. Neuroradiology. 2023;65(3):551-557. doi:10.1007/s00234-022-03073-x

70. Qin Y, Li X, Qiao Y, et al. DTI-ALPS: An MR biomarker for motor dysfunction in patients with subacute ischemic stroke. Front Neurosci. 2023;17:1132393. doi:10.3389/fnins.2023.1132393

71. Taoka T, Ito R, Nakamichi R, et al. Diffusion-weighted image analysis along the perivascular space (DWI–ALPS) for evaluating interstitial fluid status: age dependence in normal subjects. Jpn J Radiol. 2022;40(9):894-902. doi:10.1007/s11604-022-01275-0

72. Siow TY, Toh CH, Hsu JL, et al. Association of sleep, neuropsychological performance, and gray matter volume with glymphatic function in community-dwelling older adults. Neurology. 2022;98(8):e829-e838. doi:10.1212/WNL.0000000000013215

73. Zhang X, Wang W, Zhang X, et al. Normal glymphatic system function in patients with new daily persistent headache using diffusion tensor image analysis along the perivascular space. Headache. 2023;63(5):663-671. doi:10.1111/head.14514

74. McKnight CD, Trujillo P, Lopez AM, et al. Diffusion along perivascular spaces reveals evidence supportive of glymphatic function impairment in Parkinson disease. Parkinsonism Relat Disord. 2021;89:98-104. doi:10.1016/j.parkreldis.2021.06.004

75. Si X, Guo T, Wang Z, et al. Neuroimaging evidence of glymphatic system dysfunction in possible REM sleep behavior disorder and Parkinson's disease. NPJ Parkinsons Dis. 2022;8(1):54. doi:10.1038/s41531-022-00316-9

76. Qin Y, He R, Chen J, et al. Neuroimaging uncovers distinct relationships of glymphatic dysfunction and motor symptoms in Parkinson's disease. J Neurol. 2023;270(5):2649-2658. doi:10.1007/s00415-023-11594-5

77. Ozsahin I, Zhou L, Wang X, et al. Diffusion tensor imaging along perivascular spaces (DTI-ALPS) to assess effects of age, sex, and head size on interstitial fluid dynamics in healthy subjects. J Alzheimers Dis Rep. 2024;8(1):355-361. doi:10.3233/ADR-230143

78. Hsiao WC, Chang HI, Hsu SW, et al. Association of cognition and brain reserve in aging and glymphatic function using diffusion tensor image along the perivascular space (DTI-ALPS). Neuroscience. 2023;1:524:11-20. doi:10.1016/j.neuroscience.2023.04.004

79. Zhang Y, Zhang R, Ye Y, et al. The influence of demographics and vascular risk factors on glymphatic function measured by diffusion along perivascular space. Front Aging Neurosci. 2021;13:693787. doi:10.3389/fnagi.2021.693787

80. Kim J, Lee DA, Lee H, et al. Glymphatic system dysfunction in patients with cluster headache. Brain Behav. 2022;12(6). doi:10.1002/brb3.2631

81. Wang J, Zhou Y, Zhang K, et al. Glymphatic function plays a protective role in ageing-related cognitive decline. Age Ageing. 2023;52(7):1-8. doi:10.1093/ageing/afad107

82. Lee DA, Lee H, Park KM. Glymphatic dysfunction in isolated REM sleep behavior disorder. Acta Neurol Scand. 2022;145(4):464-470. doi:10.1111/ane.13573

83. Cacciaguerra L, Carotenuto A, Pagani E, et al. Magnetic resonance imaging evaluation of perivascular space abnormalities in neuromyelitis optica. Ann Neurol. 2022;92(2):173-183. doi:10.1002/ana.26419

84. Heo CM, Lee DA, Park KM, et al. Glymphatic system dysfunction in patients with early chronic kidney disease. Front Neurol. 2022;13:976089. doi:10.3389/fneur.2022.976089

85. Heo CM, Lee WH, Park BS, et al. Glymphatic dysfunction in patients with end-stage renal disease. Front Neurol. 2022;12:809438. doi:10.3389/fneur.2021.809438

86. Lee DA, Park BS, Park S, Lee YJ, Ko J, Park KM. Glymphatic system function in patients with transient global amnesia. J Integr Neurosci. 2022;21(4):117. doi:10.31083/j.jin2104117

87. Thal DR, Rüb U, Orantes M, Braak H. Phases of Aβ-deposition in the human brain and its relevance for the development of AD. Neurology. 2002;58(12):1791-1800. doi:10.1212/WNL.58.12.1791

88. Wright AM, Wu YC, Chen NK, Wen Q. Exploring radial asymmetry in MR diffusion tensor imaging and its impact on the interpretation of glymphatic mechanisms. J Magn Reson Imaging. 2023;60(4):1432-1441. doi:10.1002/jmri.29203

89. Drenthen GS, Van Der Thiel MM. Editorial for “Exploring radial asymmetry in diffusion tensor imaging and its impact on the interpretation of glymphatic mechanisms.” J Magn Reson Imaging. 2024;60(4):1442-1443. doi:10.1002/jmri.29377

9 Appendices

9.1 Appendix A – Study ethical approval

UNIVERSITÄT ZU LÜBECK

Universität zu Lübeck Ratzeburger Allee 160 23562 Lübeck

Institut für Neuroradiologie
Frau Dr. rer. nat Patricia Ulloa Almendras
Ratzeburger Allee 160
23538 Luebeck
Deutschland

Ethik-Kommission

Vorsitzender:
Herr Prof. Dr. med. Alexander Katalinic

Stellv. Vorsitzender:
Herr Prof. Dr. med. Frank Gieseler

Geschäftsstelle:
Dr. rer. nat. Inga Kaufhold +49(0)451 3101 1026
Dr. rer. nat. Christopher Link +49(0)451 3101 1009
Janine Kurzaj-Erdmann +49(0)451 3101 1008
Doris Seuthe +49(0)451 3101 1025

E-Mail: ethikkommission@uni-luebeck.de

Website: www.uni-luebeck.de/forschung/kommissionen/ethikkommission

Aktenzeichen: 2022-630
21.12.2022 / IK

Verkürztes Verfahren - Anzeige
Antragsteller: Dr. rer. nat Patricia Ulloa Almendras
Titel: Glymphatic system evaluation via MR diffusion tensor imaging along perivascular spaces in brain tumor patients
Hier: Ihr Schreiben vom 08.12.2022

Sehr geehrte Frau Ulloa Almendras,

mit Ihrem o.g. Schreiben informieren Sie die Ethik-Kommission über Ihr geplantes Vorhaben.

Die Ethik-Kommission nimmt das Vorhaben nach Berücksichtigung der folgenden Hinweise zustimmend zur Kenntnis.

Studienprotokoll:

- Die Kommission geht davon aus, dass ausschließlich vorliegende Bilder genutze werden und keine neuen Untersuchungen/Messungen durchgeführt werden

- S. 4: Als Einschlusskriterium ist das Alter (>18 Jahre) zu ergänzen

- S. 4: Den Begriff pseudo-anonymisiert gibt es im Datenschutz nicht. Es ist zu beschreiben, ob die Daten pseudonymisiert oder anonymisiert erhoben und analysiert werden und wie dies erfolgt. Die Daten sind frühestmöglich zu anonymisieren.

- Patienten, die einer Verwendung ihrer Behandlungsdaten zu wissenschaftlichen Zwecken widersprochen haben, sind auszuschließen (Broad consent).

Mit freundlichen Grüßen

Prof. Dr. Alexander Katalinic
Vorsitzender der Ethik-Kommission

Allgemeine Hinweise:
Aufgeführte Hinweise sind zu berücksichtigen. Eine Wiedervorlage ist nicht nötig. Bei Bedarf eines Votums ohne Hinweise sind die angepassten Dokumente als Amendmend vorzulegen. Änderungen sind hervorzuheben.
Datenschutzrechtliche Aspekte von Forschungsvorhaben werden durch die Ethikkommission grundsätzlich nur kursorisch geprüft. Dieses Votum / diese Bewertung ersetzt mithin nicht die Konsultation des zuständigen Datenschutzbeauftragten.

B

Vorgelegte Dokumente

1) Basisformular_ethik_DTIALPS.pdf vom 08.12.2022
2) DTI-ALPS-ProjectDescription.pdf vom 08.12.2022
3) nicht verfügbar - Studieninformation und Einwilligungserklärung.pdf vom 08.12.2022
4) nicht verfügbar - vertragliche Vereinbarungen.pdf vom 08.12.2022
5) PatriciaUlloa_Cover_letter.pdf vom 08.12.2022
6) Unterschriftenblatt.pdf vom 08.12.2022

C

UNIVERSITÄT ZU LÜBECK

Universität zu Lübeck Ratzeburger Allee 160 23562 Lübeck

Institut für Neuroradiologie
Frau Dr. rer. nat Patricia Ulloa Almendras
Ratzeburger Allee 160
23538 Luebeck
Deutschland

Ethik-Kommission

Vorsitzender:
Herr Prof. Dr. med. Alexander Katalinic

Stellv. Vorsitzender:
Herr Prof. Dr. med. Andreas Moser

Geschäftsstelle:
Dr. rer. nat. Inga Kaufhold +49(0)451 3101 1026
Dr. rer. nat. Christopher Link +49(0)451 3101 1009
Corinna Bürgel +49(0)451 3101 1027
Doris Seuthe +49(0)451 3101 1025

E-Mail: ethikkommission@uni-luebeck.de

Website: www.uni-luebeck.de/forschung/kommissionen/ethikkommission

Aktenzeichen: 2022-630_1
18.01.2024 / IK

Verkürztes Verfahren - Amendment
Antragsteller: Dr. rer. nat Patricia Ulloa Almendras
Titel: Glymphatic system evaluation via MR diffusion tensor imaging along perivascular spaces in brain tumor patients
Hier: Ihre Einreichung vom 11.01.2024, Einschluss gesunder Kontrollen aus 2023-416

Sehr geehrte Frau Dr. rer. nat Patricia Ulloa Almendras,

Die Ethik-Kommission nimmt die nachträglichen Änderungen zustimmend zur Kenntnis

Mit freundlichen Grüßen

Prof. Dr. Alexander Katalinic
Vorsitzender der Ethik-Kommission

Allgemeine Hinweise:
Ggf. aufgeführte Hinweise sind zu berücksichtigen. Eine Wiedervorlage ist nicht nötig. Bei Bedarf eines Votums ohne Hinweise sind die angepassten Dokumente als Amendmend vorzulegen. Änderungen sind hervorzuheben.
Datenschutzrechtliche Aspekte von Forschungsvorhaben werden durch die Ethikkommission grundsätzlich nur kursorisch geprüft. Dieses Votum / diese Bewertung ersetzt mithin nicht die Konsultation des zuständigen Datenschutzbeauftragten.

Vorgelegte Dokumente
1) pu240111_DTI-ALPS-ProjectDescription_HC.pdf vom 11.01.2024

9.2 Appendix B – Patient information

Table with complete patient information

Table 2 Demographic information. *Patient nr. 5 was referred from another institution, ^{ROI} means that the ROI was placed in the PTBE

Patient nr.	Age	Sex	DTI ALPS ipsilateral	DTI ALPS contralateral	Tumor's ADC $mm^2\ s^{-1}$	Event	Type of tumor	Details	Tumor location	PTBE
1	24	Male	1.10	1.37	1601	Local recurrence	Primary	Diffuse Astrocytoma	Left frontal	No
2	73	Female	0.98	1.18	525.5	Distant recurrence	Metastasis	B-cell lymphoma	Left high frontal	No
3	71	Female	1.0	1.21	75.5	Distant recurrence	Metastasis	Bronchial carcinoma	Left high frontal	Yes^{ROI}
4	68	Female	1.12	1.31	810	Distant recurrence	Metastasis	Mammary carcinoma	Left occipital	Yes
5	48	Male	1.14	1.15	1220	First diagnosis	Primary	Unclear*	Left temporofronto-parieto insular	Yes^{ROI}
6	56	Female	Excluded							
7	38	Male	0.96	1.30	1287	Local recurrence	Primary	Glioblastoma	Left frontal	Yes^{ROI}
8	59	Male	Excluded							
9	53	Male	1.67	1.81	1558	First diagnosis	Primary	Diffuse Astrocytoma	Left temporoinsular	Yes
10	51	Male	1.39	1.51	1333	Local recurrence	Primary	Diffuse Astrocytoma	Right frontotemporoinsular	No
11	51	Male	1.34	1.58	1291	Local recurrence	Primary	Diffuse Astrocytoma	Right frontotemporoinsular	No
12	56	Female	2.03	2.28	1719	First diagnosis	Primary	Convexity meningioma	Left convexity	No
13	71	Male	1.29	1.30	1845	Local recurrence	Primary	Glioblastoma	Left temporal	Yes
14	72	Female	Excluded							

15	67	Female	1.54	1.44	2688	Distant recurrence	Metastasis	Clear cell renal carcinoma	Left temporal	Yes
16	60	Female	1.13	1.59	2734	Local recurrence	Primary	Multifocal glioblastoma	Left parietooccipital and left occipital	Yes
17	67	Female	1.35	1.35	2883	Distant recurrence	Metastasis	Renal cell carcinoma	Left parietooccipital	Yes
18	43	Male	1.28	1.62	1769	Distant recurrence	Metastasis	Bronchial carcinoma	Left temporal	Yes
19	62	Female	Excluded							
20	70	Male	1.42	1.58	1556	First diagnosis	Primary	Glioblastoma	Right high frontal	Yes
21	58	Male	1.20	1.22	1140	First diagnosis	Primary	Glioblastoma	Left temporal	Yes
22	61	Female	1.01	1.19	1798	Local recurrence	Primary	Multifocal glioblastoma	Left parietoocipital and left occipital	Yes
23	57	Male	1.18	1.32	2057	Local recurrence	Primary	Glioblastoma	Left temporoinsular	Yes[ROI]
24	61	Female	Excluded							
25	50	Male	1.34	1.55	2257	Local recurrence	Primary	Oligodendroglioma grade III	Left parietal	Yes
26	54	Male	Excluded							
27	32	Male	1.30	1.40	1576	First diagnosis	Primary	Oligodendroglioma grade II	Left frontal	Yes
28	58	Female	1.16	1.17	1059.5	Distant recurrence	Metastasis	Bronchial carcinoma	Left parietal and left occipital	Yes
29	59	Female	1.24	1.89	1628	Local recurrence	Primary	Glioblastoma	Left temporoparieto-occipital	Yes[ROI]
30	72	Male	1.03	1.25	2444	First diagnosis	Primary	Glioblastoma	Left temporal	Yes

9.3 Appendix C – ROI positioning: Patients

Regions-of-interest positioning in included patients

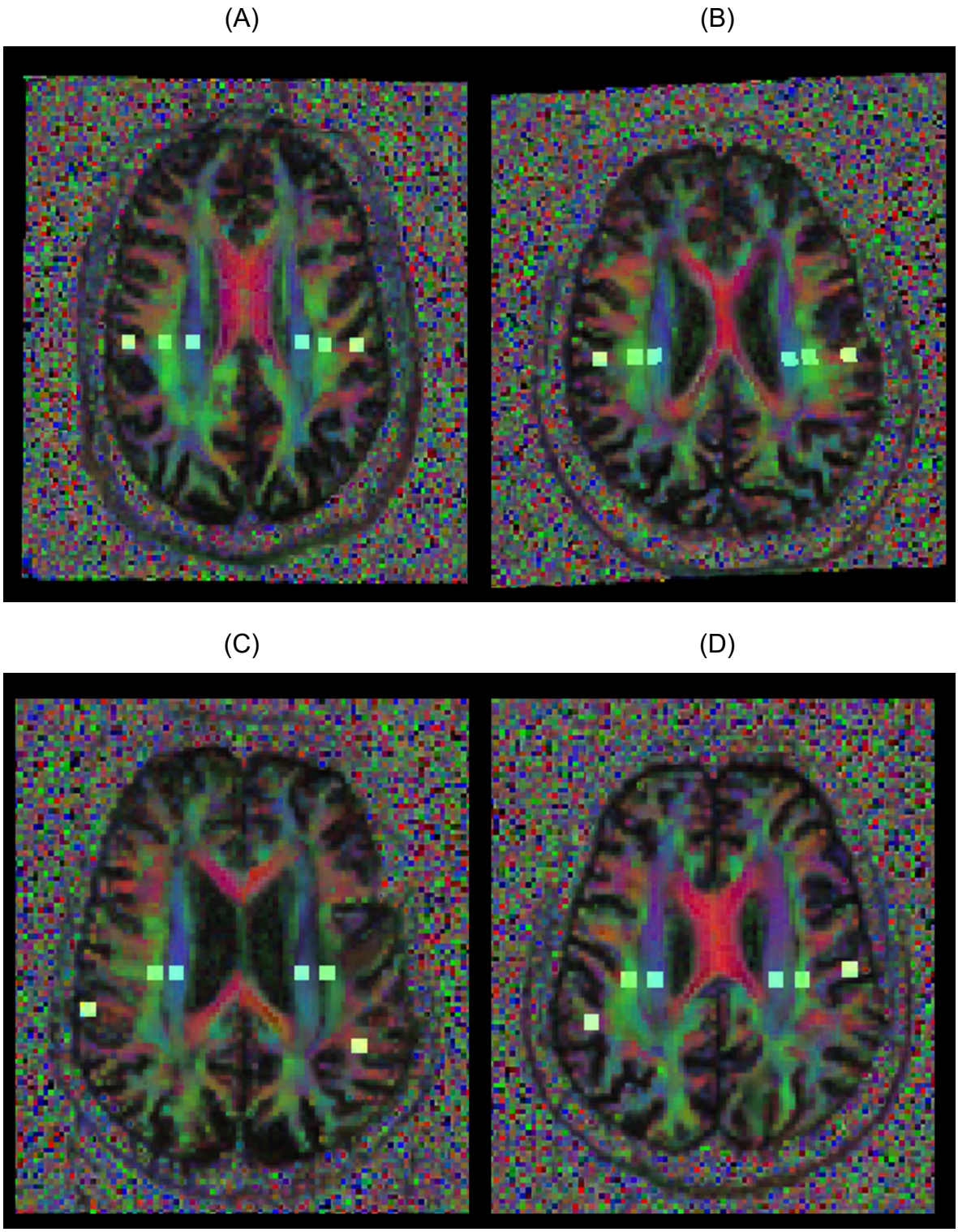

Figure B.a (A) Patient 1, male, 24 years old, astrocytoma. (B) Patient 2, female, 73 years old, B Cell lymphoma. (C) Patient 3, female, 71 years old, bronchial carcinoma. (D) Patient 4, female, 68 years old, breast carcinoma

(A) (B)

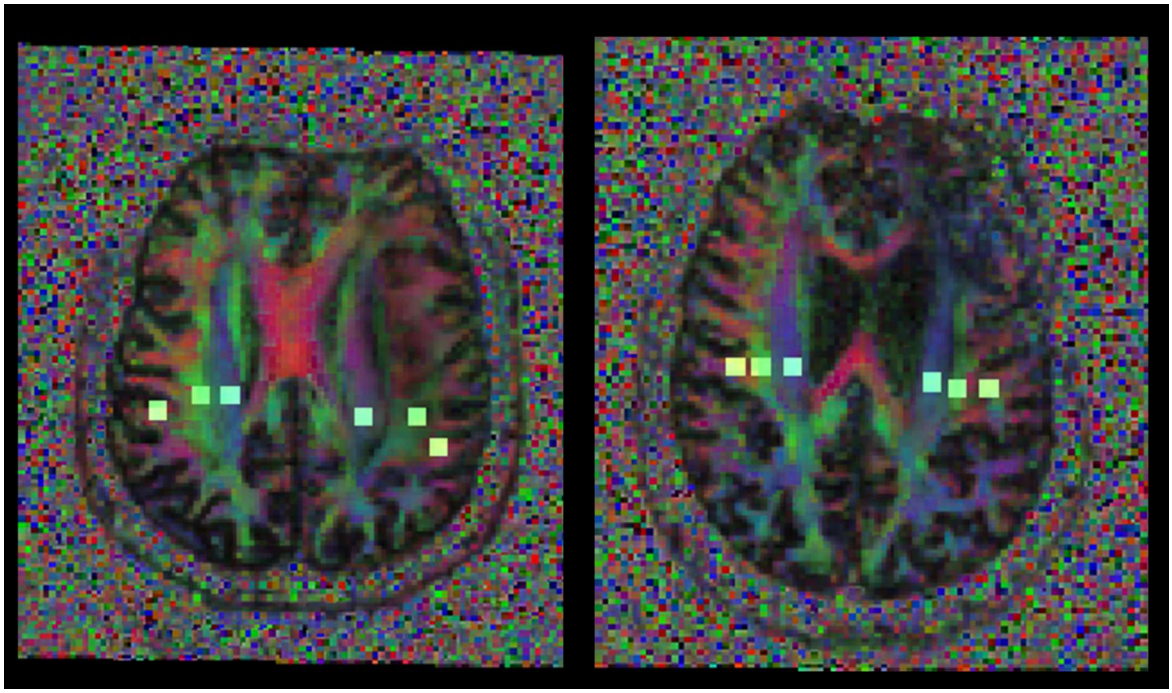

(C) (D)

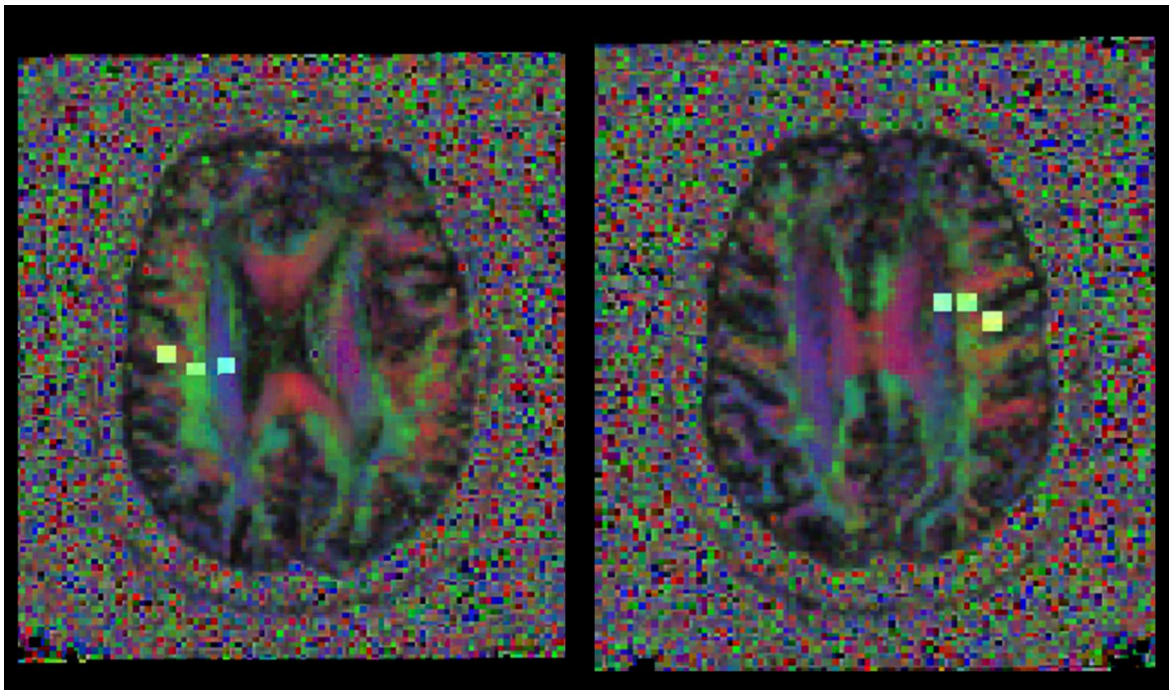

Figure B.b (A) Patient 5, male, 48 years old, unclear. (B) Patient 7, male, 38 years old, astrocytoma. (C) and (D) Patient 9, male, 53 years old, astrocytoma, right and left hemisphere, respectively.

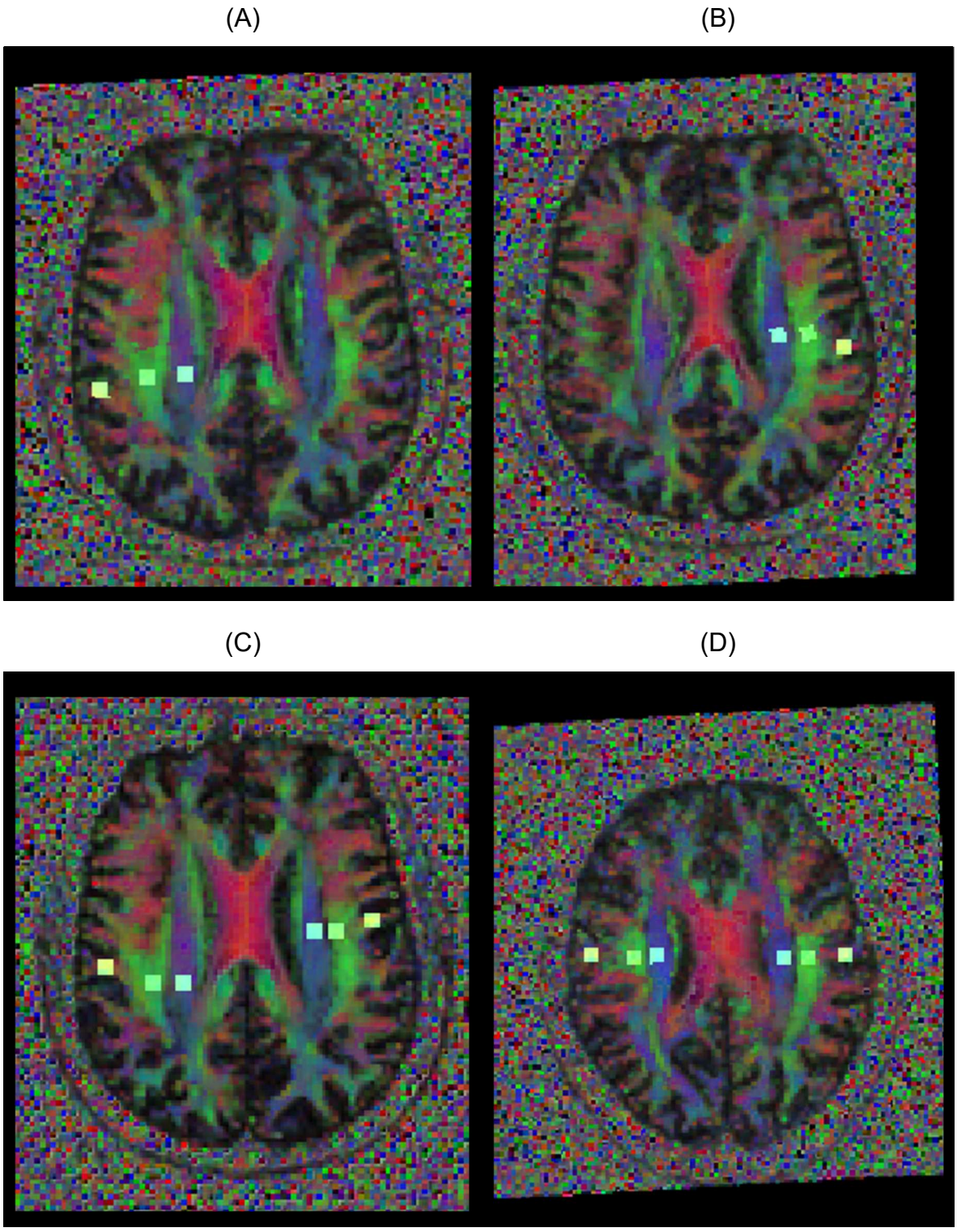

Figure B.c (A) and (B) Patient 10, male, 51 years old, astrocytoma, right and left hemisphere, respectively. (C) Patient 11, male, 51 years old, Astrocytoma. (D) Patient 12, female, 56 years old, meningioma.

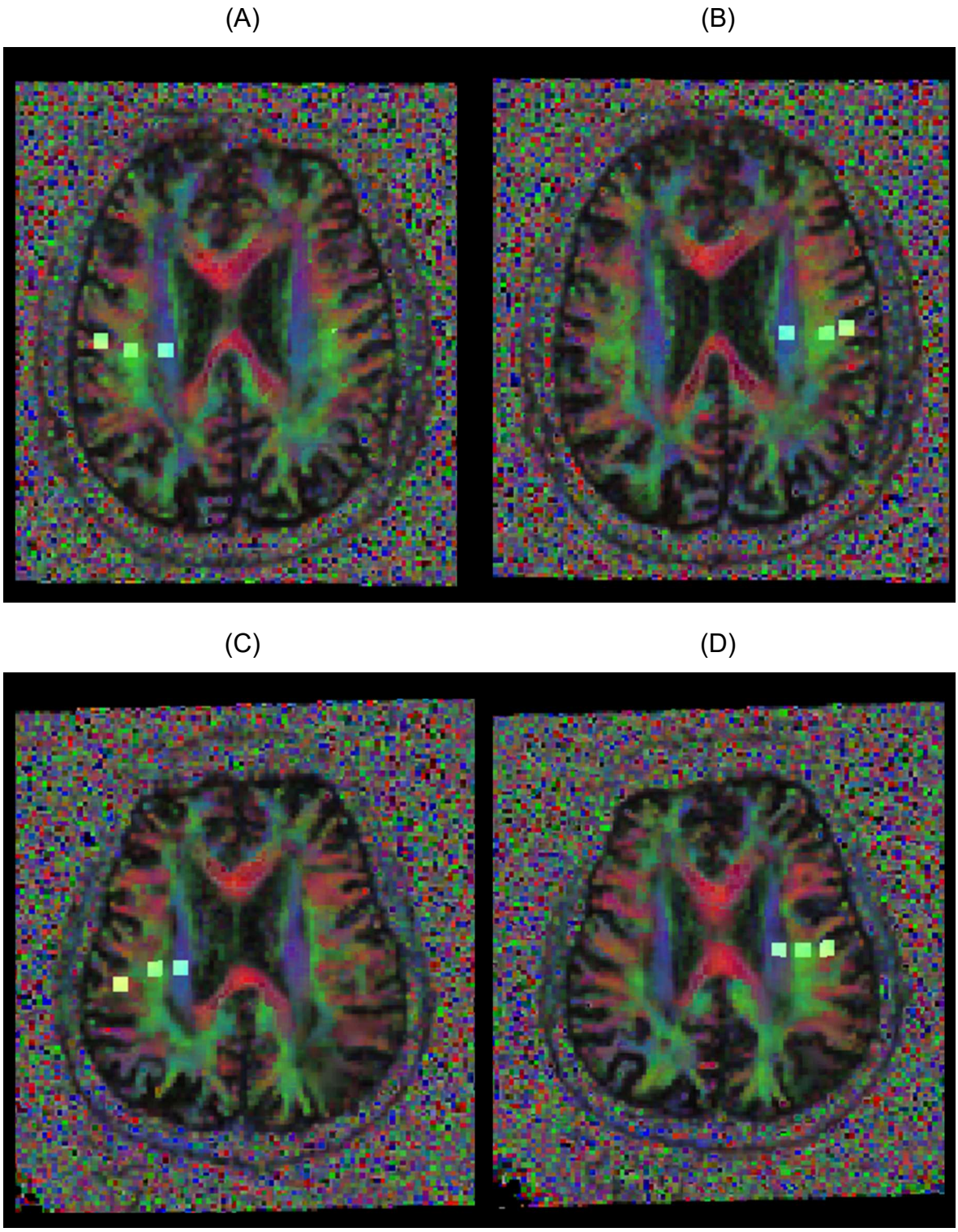

Figure B.d (A) and (B) Patient 13, male, 71 years old, glioblastoma, right and left hemisphere, respectively. (C) and (D) Patient 15, female, 67 years old, kidney clear cell carcinoma right and left hemisphere, respectively.

L

(A) (B)

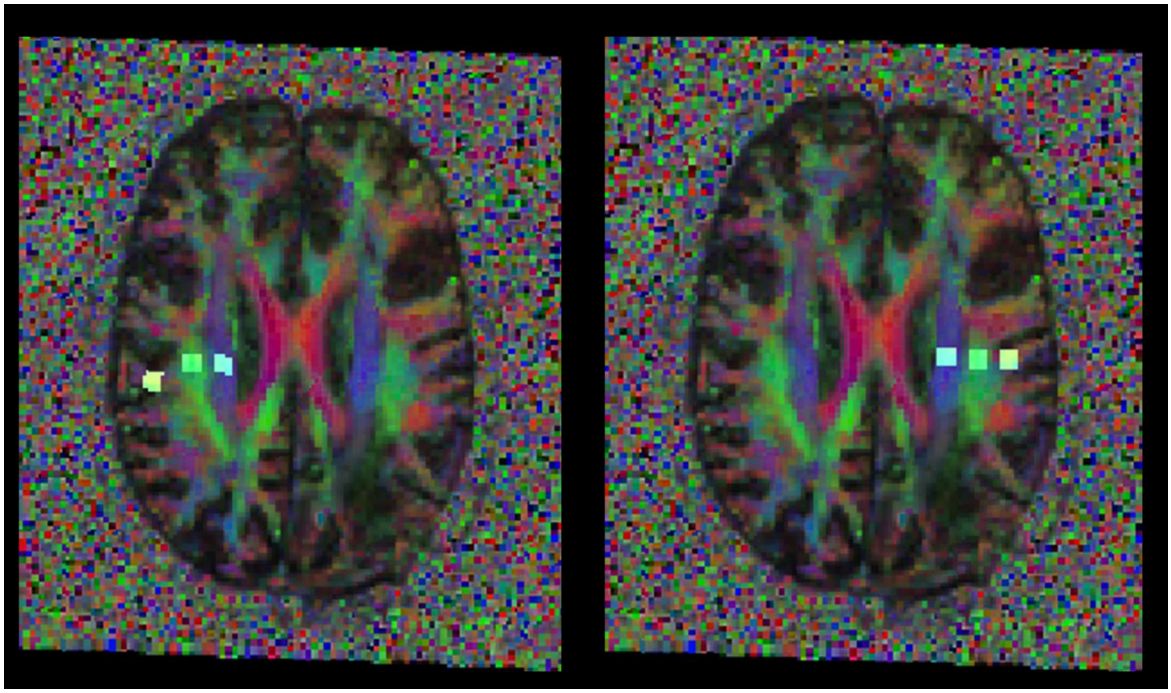

(C) (D)

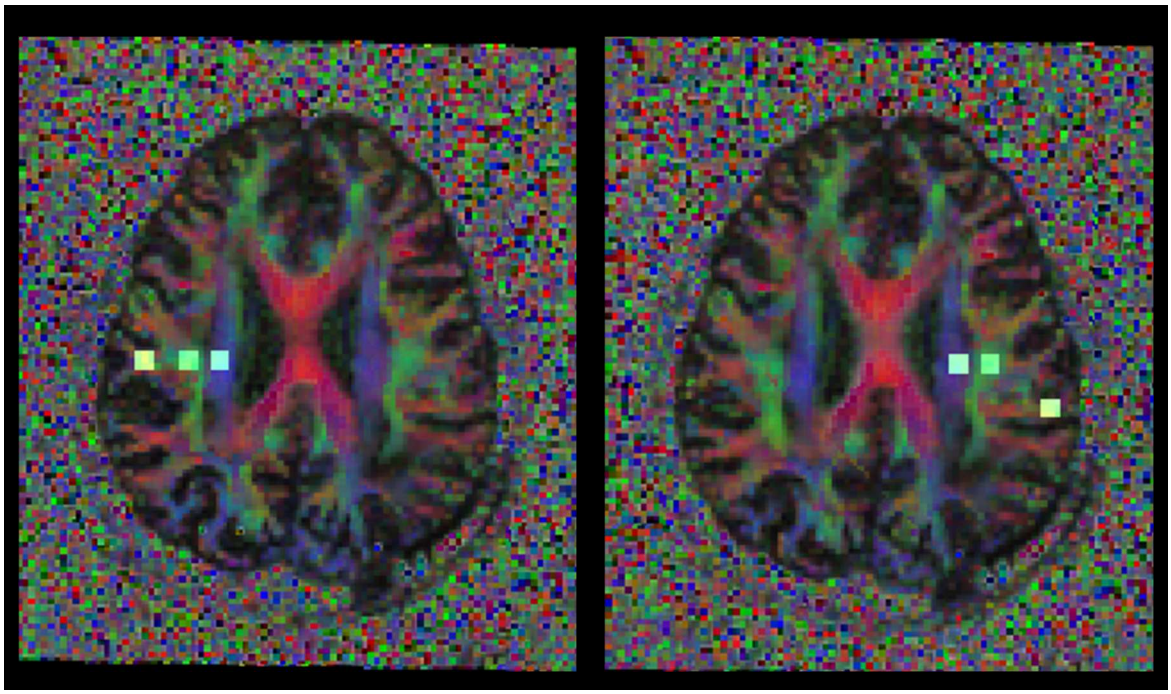

Figure B.e (A) and (B) Patient 16, female 60 years old, glioblastoma, right and left hemisphere, respectively. (C) and (D) Patient 17, female, 67 years old, renal cell carcinoma, right and left hemisphere, respectively.

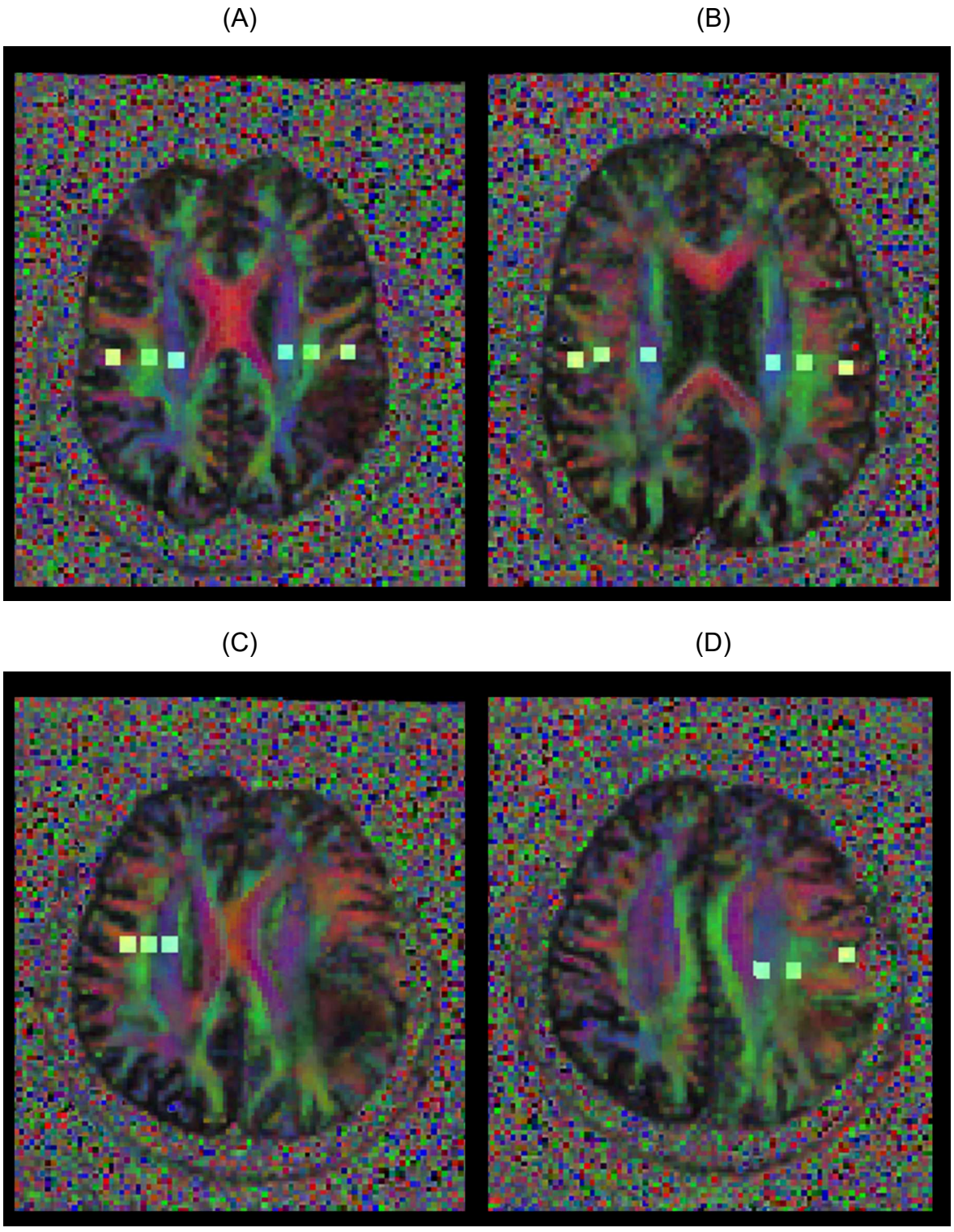

Figure B.f (A) Patient 18, male, 43 years old, bronchial carcinoma. (B) Patient 20, male, 70 years old, glioblastoma. (C) and (D) Patient 21, male, 58 years old, glioblastoma right and left hemisphere, respectively.

(A) (B)

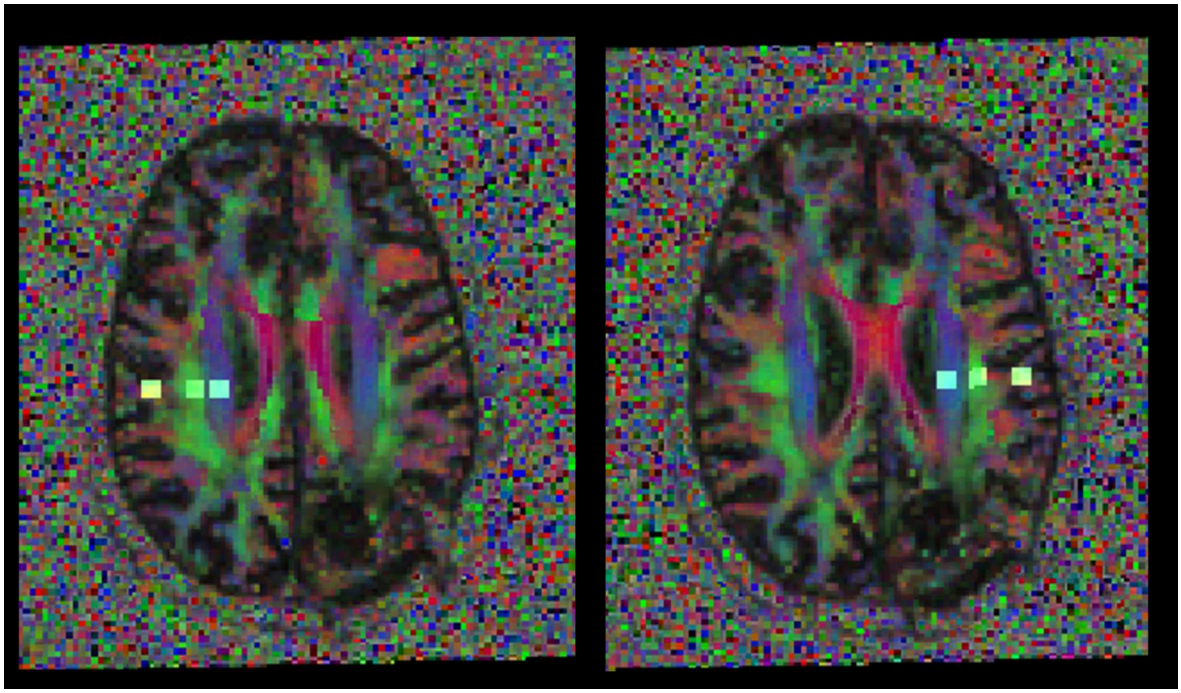

(C) (D)

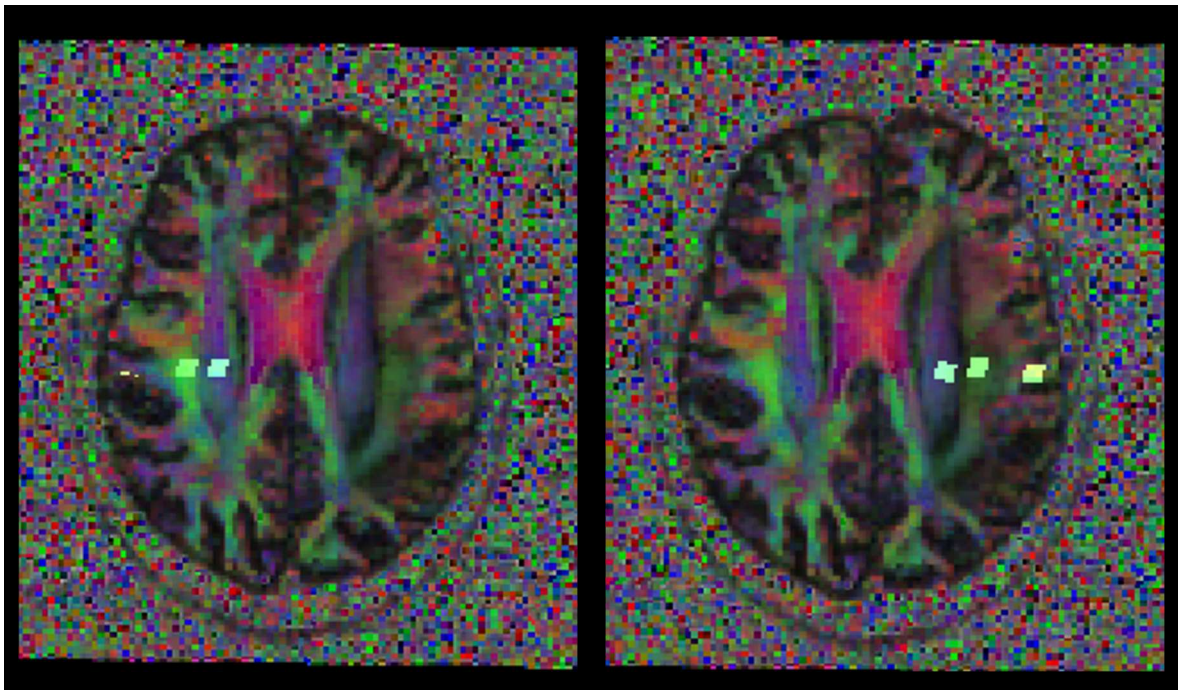

Figure B.g (A) and (B) Patient 22, female, 61 years old, glioblastoma right and left hemisphere, respectively. (C) and (D) Patient 23, male, 57 years old, glioblastoma, right and left hemisphere, respectively.

(A) (B)

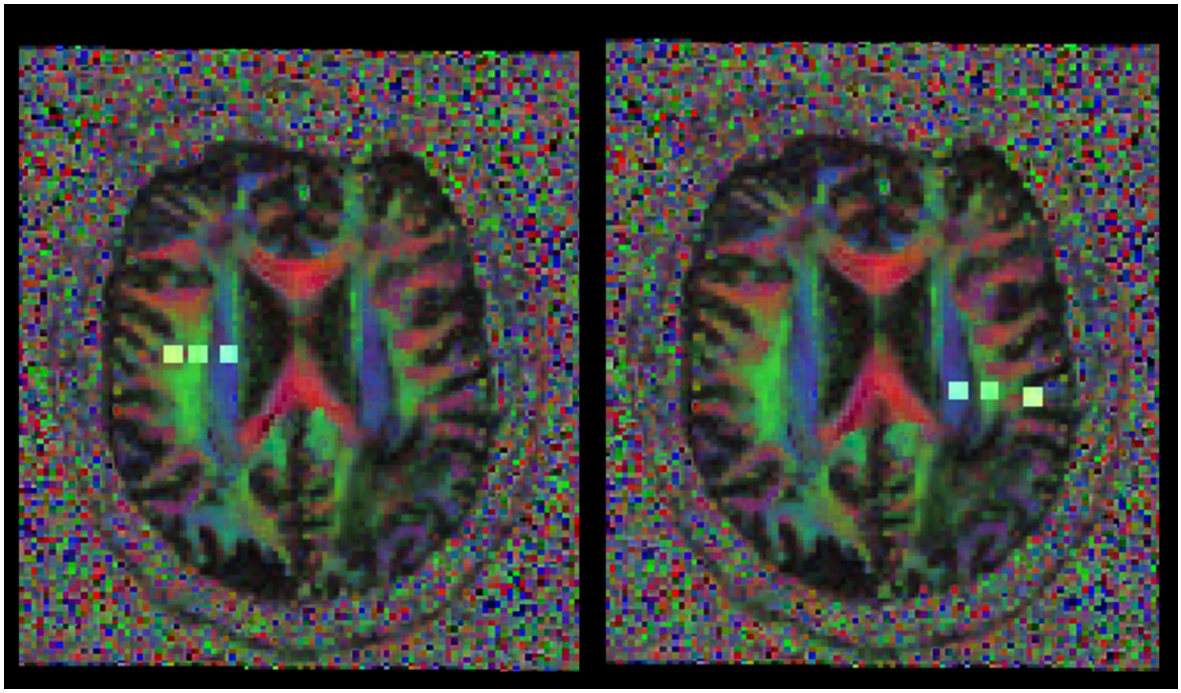

(C) (D)

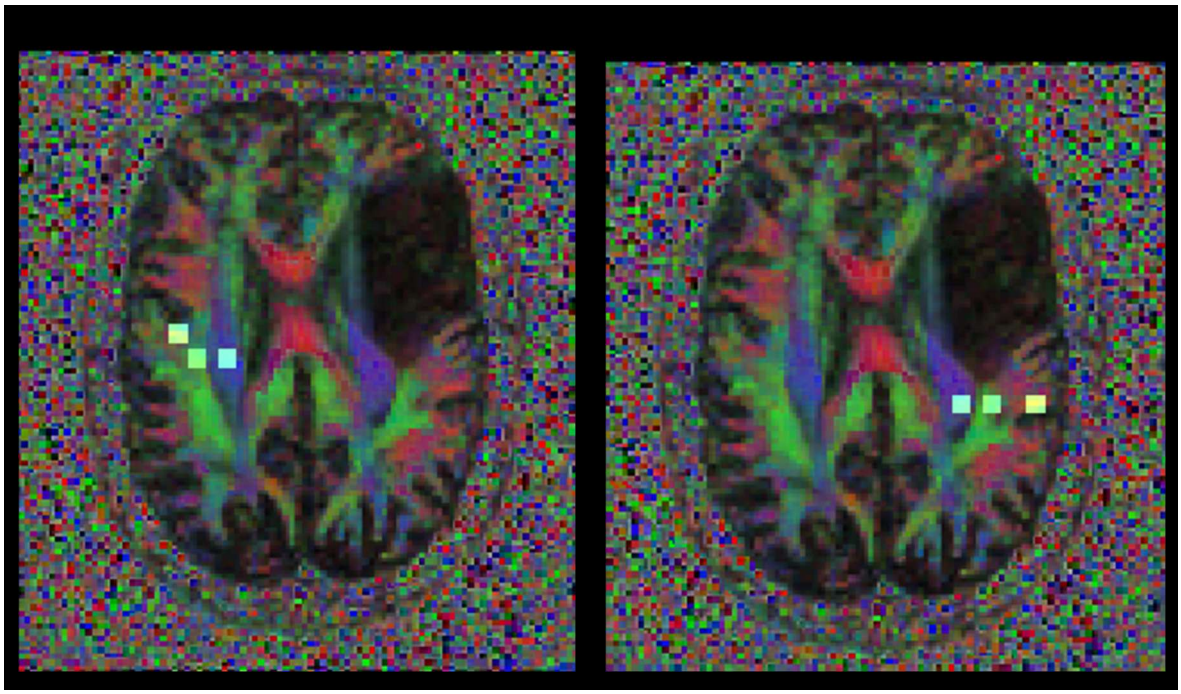

Figure B.h (A) and (B) Patient 25, male, 50 years old, oligodendroglioma, right and left hemisphere respectively. (C) and (D) Patient 27, male 32 years old, oligodendroglioma, right and left hemisphere, respectively.

(A)

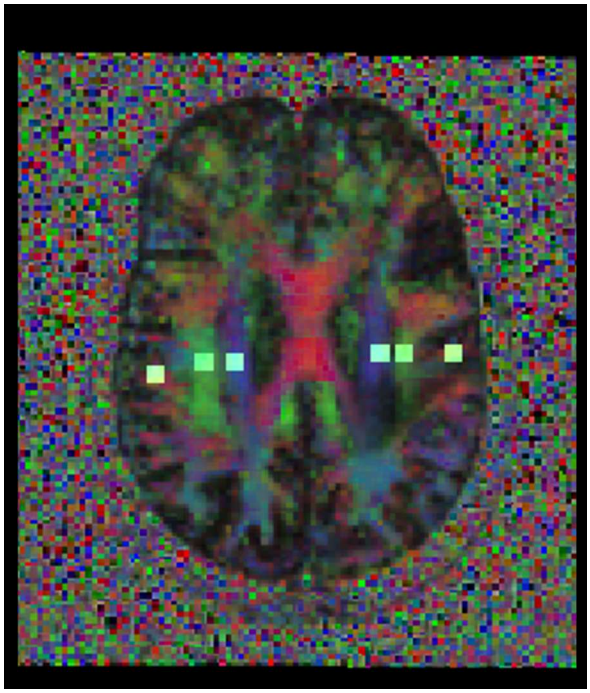

(B) (C)

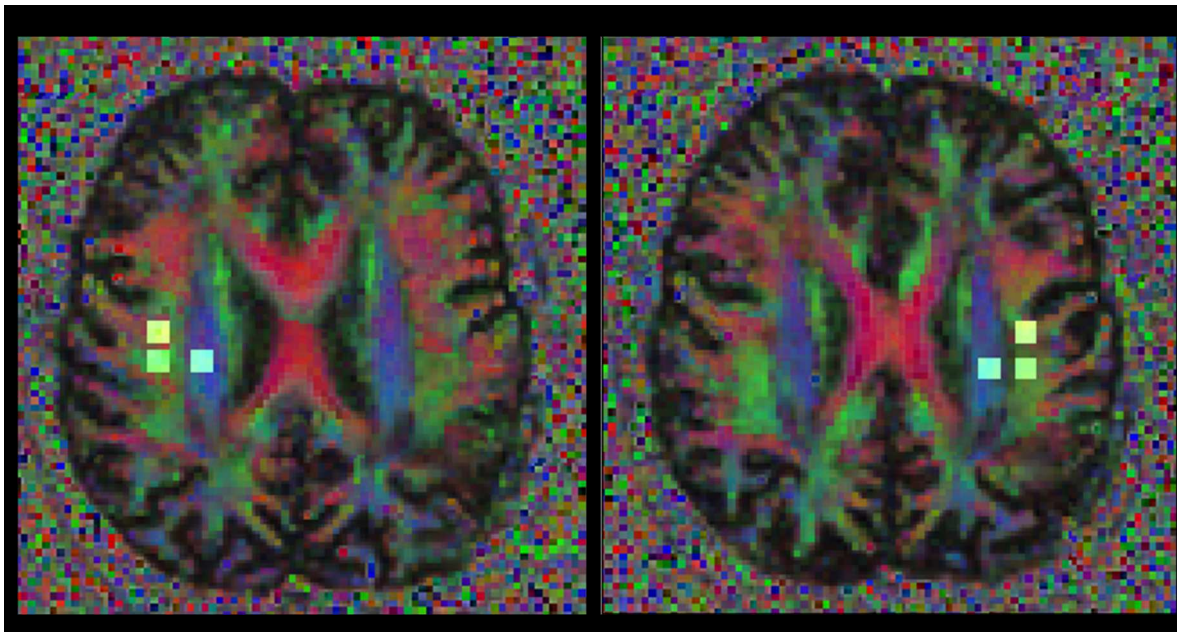

Figure B.i (A) Patient 28, female, 58 years old, bronchial carcinoma. (B) and (C) Patient 29, female, 59 years old, glioblastoma, right and left hemisphere, respectively

Q

(A) (B)

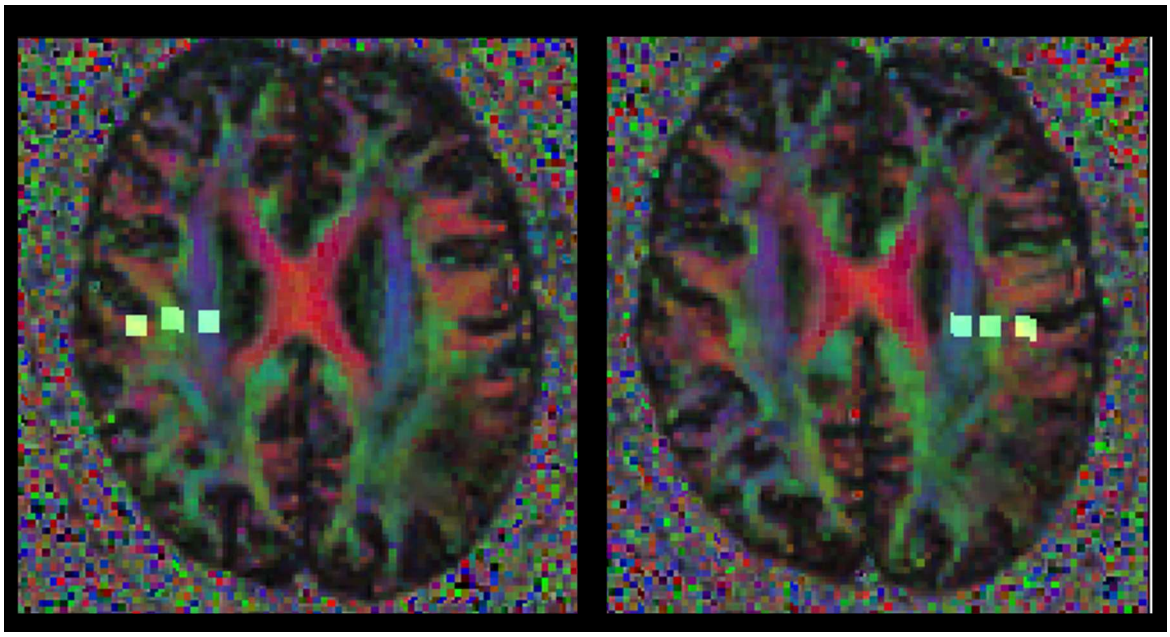

Figure B.j (A) and (B) Patient 30, male, 72 years old, glioblastoma, right and left hemisphere, respectively.

R

9.4 Appendix D – ROI positioning: Healthy controls

Region-of-interest positioning in healthy controls

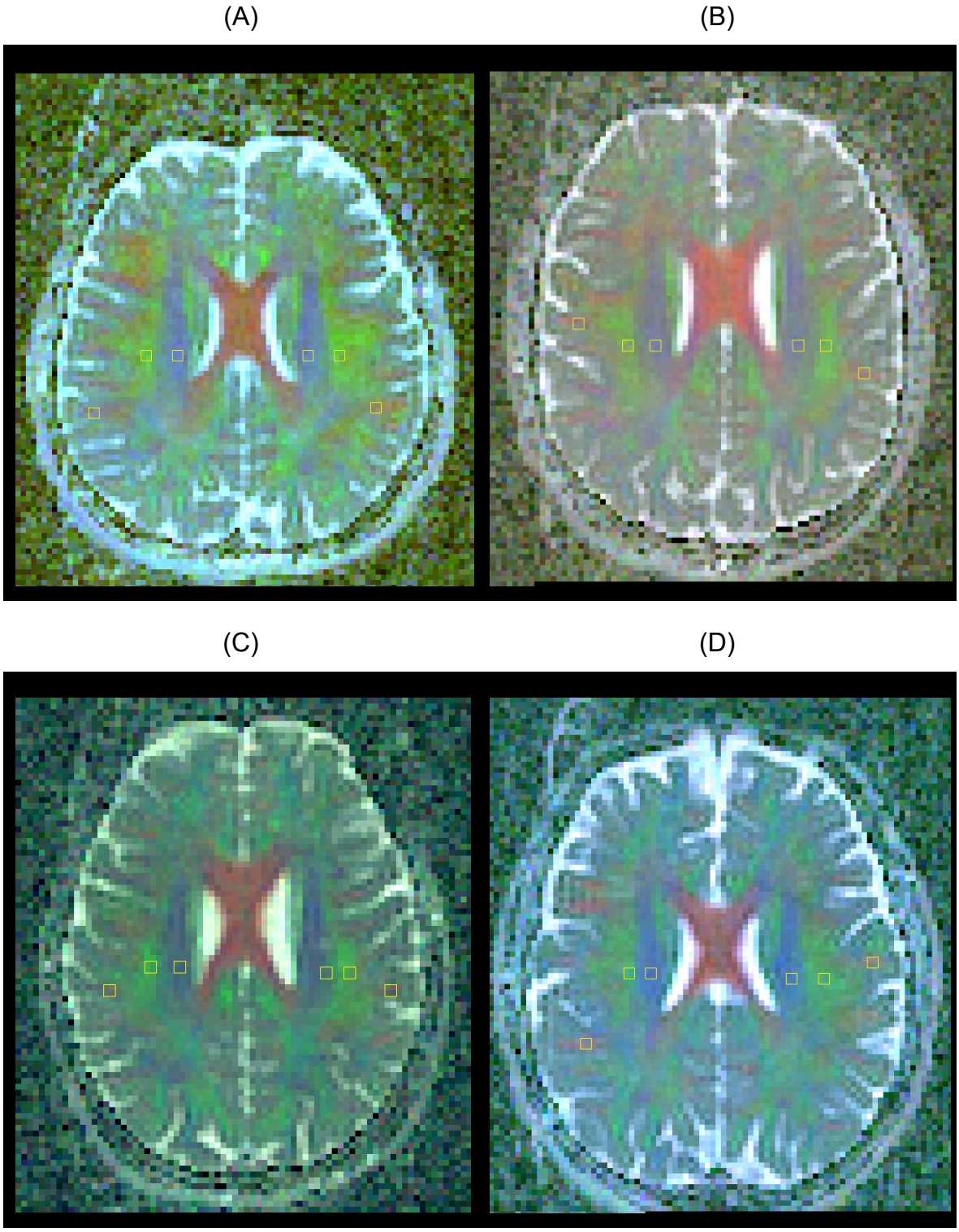

Figure D.a (A) Male, 33 years old. (B) Male, 24 years old. (C) Female, 57 years old. (D) Male, 59 years old.

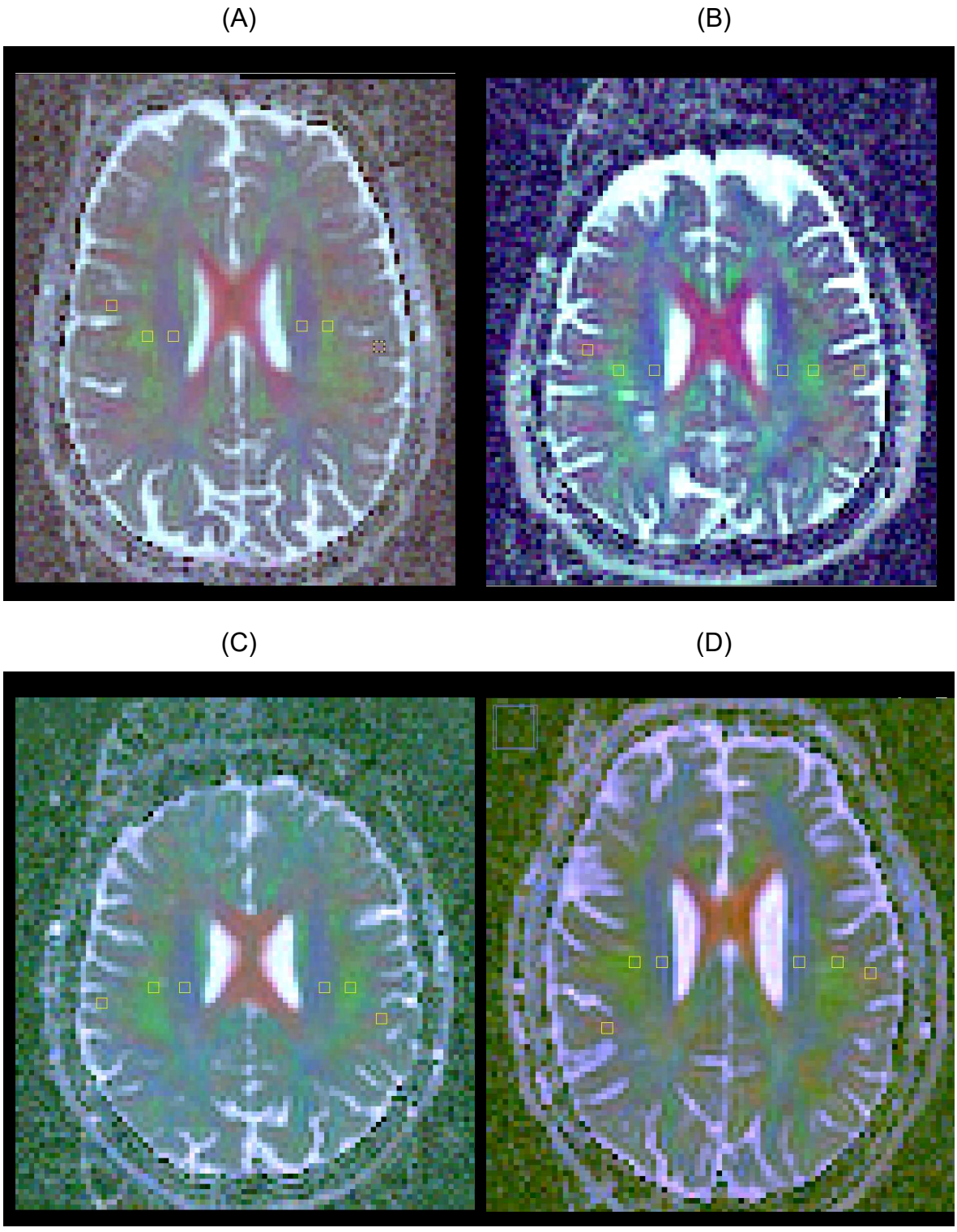

Figure D.b (A) Male, 41 years old. (B) Male, 70 years old. (C) Female, 66 years old. (D) Male, 48 years old.

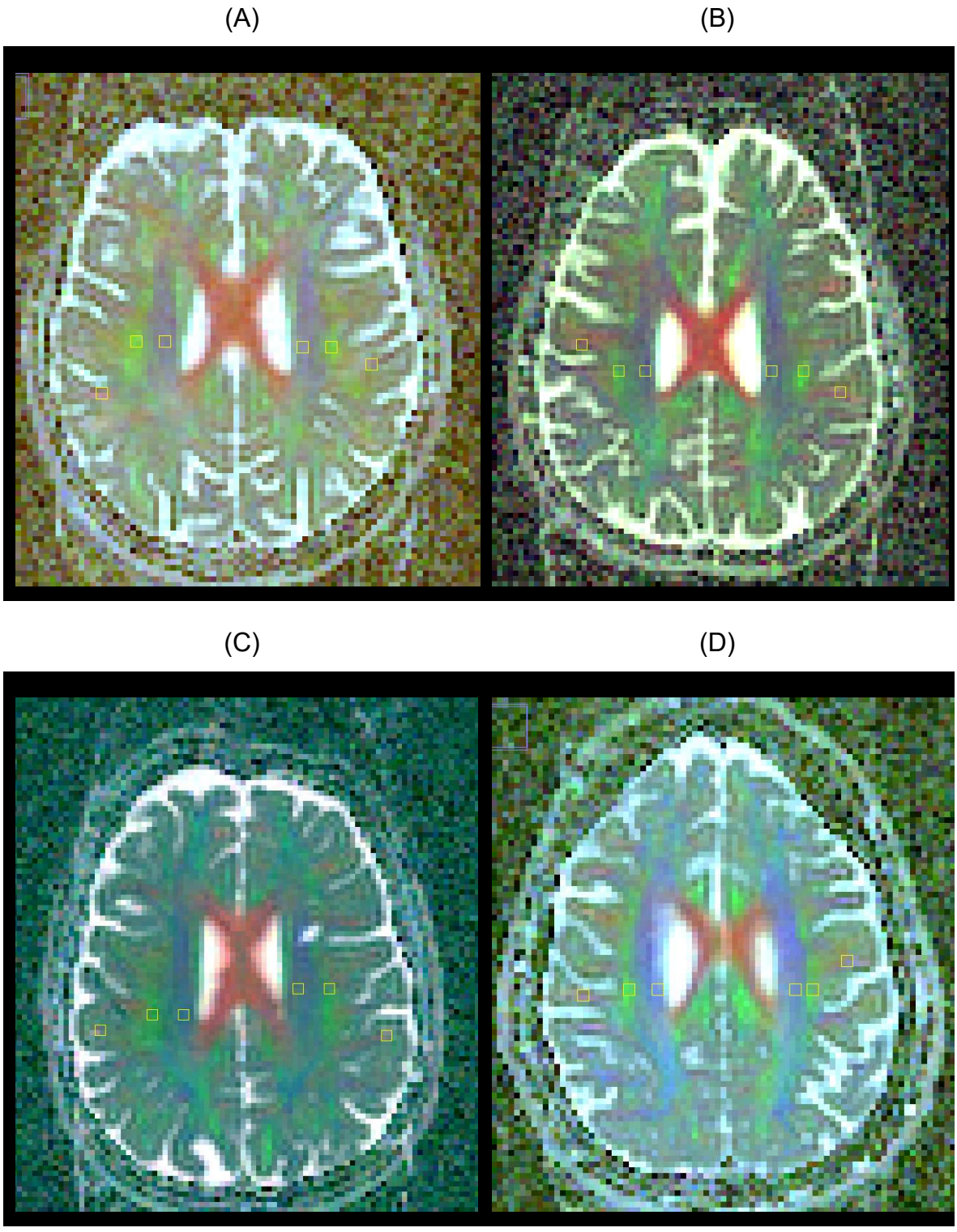

Figure D.c (A) Female, 71 years old. (B) Female, 61 years old. (C) Male, 43 years old. (D) Male, 52 years old.

9.5 Appendix E – Healthy control information

Table 3 Information for matched healthy controls

Control no.	Sex	Age / years	DTI ALPS Right hem.	DTI ALPS Left hem.	Matched patient
1	m	33	1.51	1.52	27
2	m	24	1.52	1.31	1
3	f	57	1.38	1.39	12, 16, 28, 29
4	m	59	1.31	1.31	21, 23
5	m	41	1.45	1.47	7
6	m	70	0.90	0.85	13, 20, 30
7	f	67	1.37	1.46	4, 15, 17
8	m	49	1.23	1.14	5
9	f	71	1.42	1.25	2, 3
10	f	61	0.88	0.93	22
11	m	43	1.51	1.42	18
12	m	52	0.99	1.09	25, 10, 11, 9
mean ± std		52.25 ± 14.20	1.29 ± 0.23	1.26 ± 0.21	
median (Q1, Q3)		54 (42.50, 62.5)	1.37 (1.17, 1.46)	1.31 (1.13, 1.43)	

DTI ALPS, diffusion-tensor imaging across the perivascular spaces; hem., hemisphere

9.6 Appendix F – Excluded patients

(A) (B)

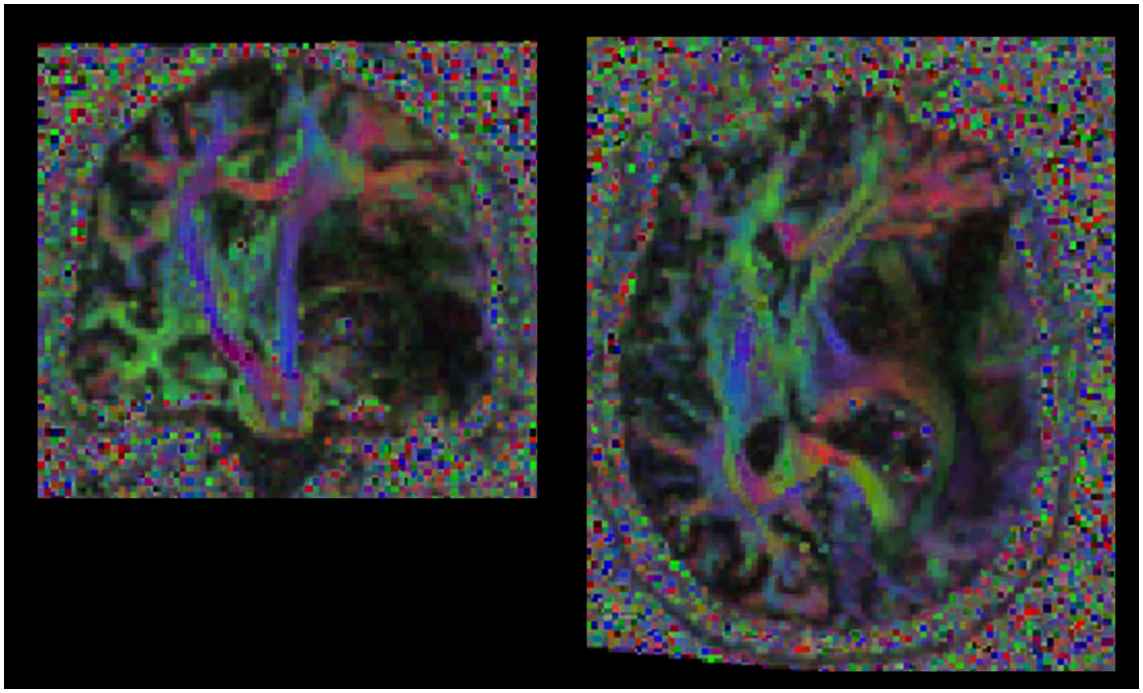

(C) (D)

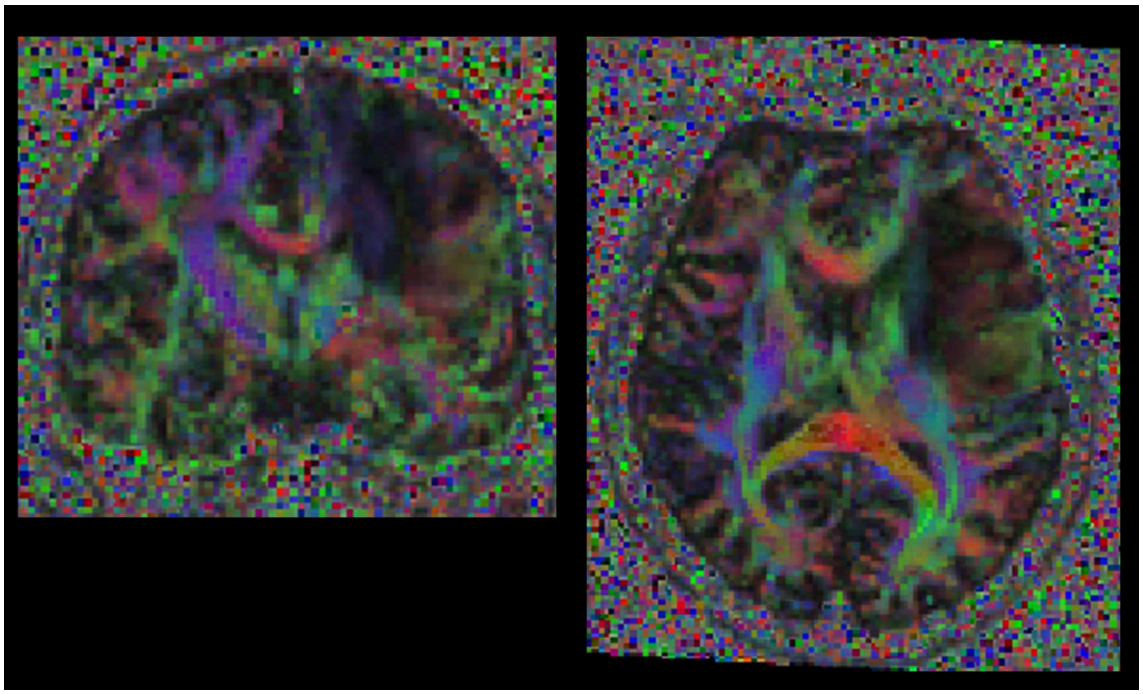

Figure C.a (A) and (B) Patient 6, female, 56 years old, breast carcinoma, coronal and axial, respectively. (C) and (D) Patient 8, male, 59 years old. B Cell lymphoma, coronal and axial, respectively.

(A) (B)

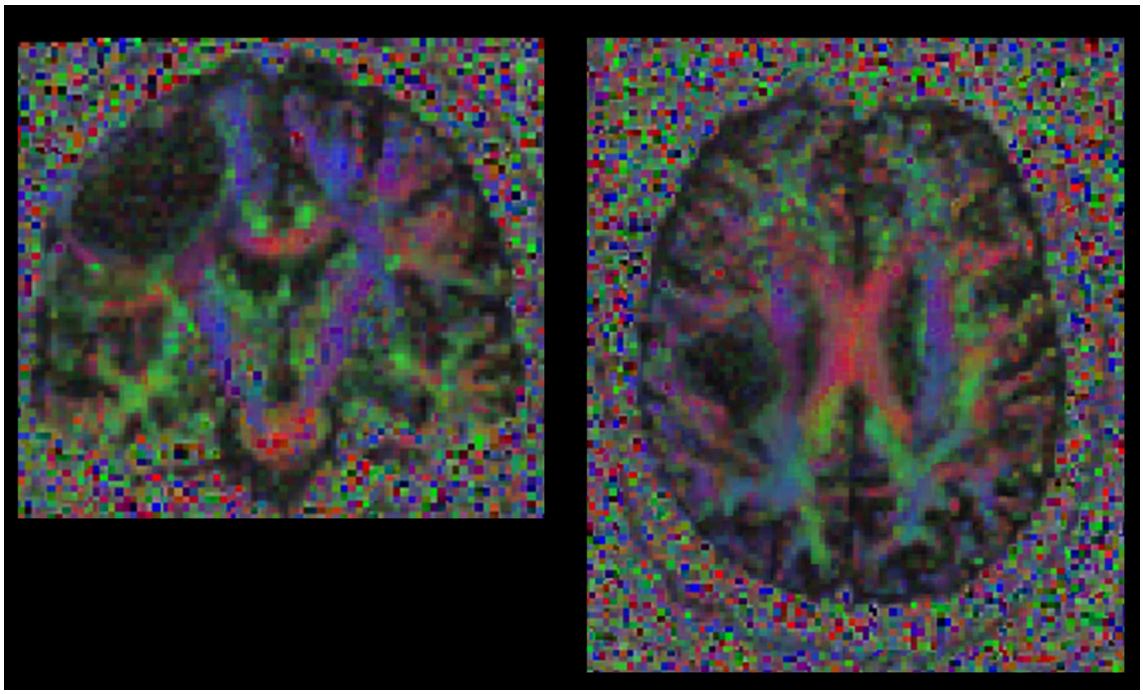

(C) (D)

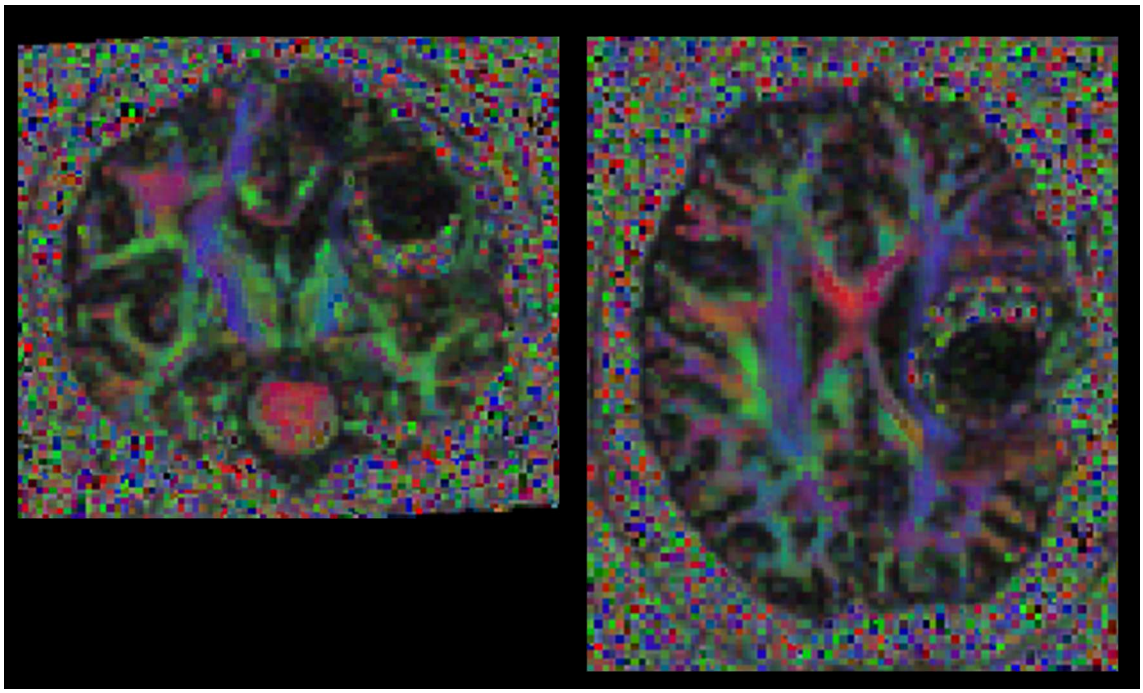

Figure C.b (A) and (B) Patient 14, female, 72 years old, endometrial adenocarcinoma, coronal and axial, respectively. (C) and (D) Patient 19, female, 62 years old, glial tumor, coronal andaxial, respectively.

(A) (B)

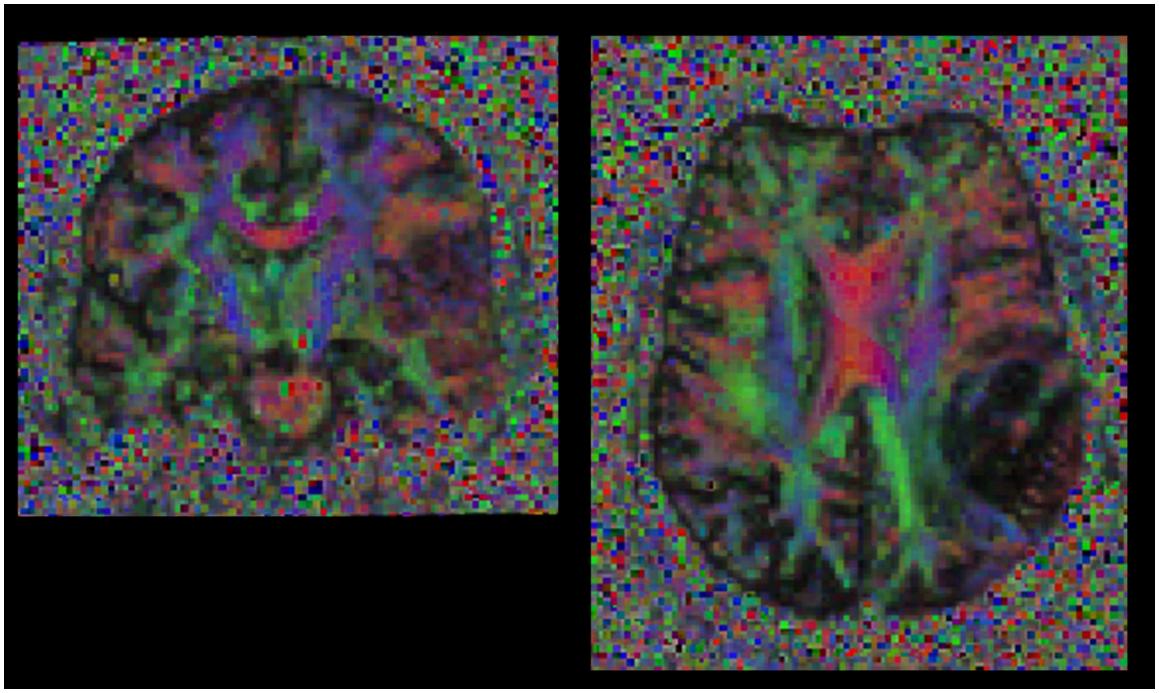

(C) (D)

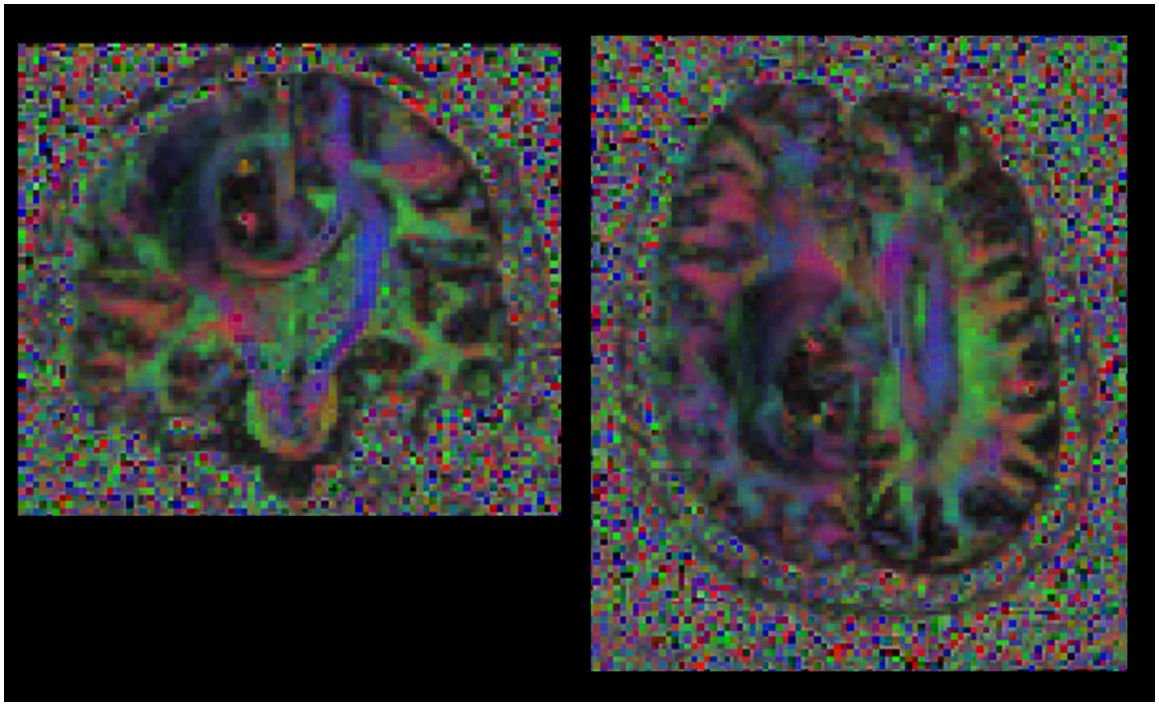

Figure C.c (A) Patient 24, female, 61 years old, glioblastoma, coronal cut. (B) Patient 24, female, 61 years old, glioblastoma, axial cut. (C) Patient 26, male, 54 years old, glioblastoma, coronal. (D) Patient 26, male, 54 years old, glioblastoma, axial

9.7 Appendix G – ROI positioning complications

We observed that in Matlab, under certain rotations, the positioning of the regions-of-interest could seem uneven. Under a higher magnification, one can observe the correct positioning, as demonstrated in the following example.

(A) (B)

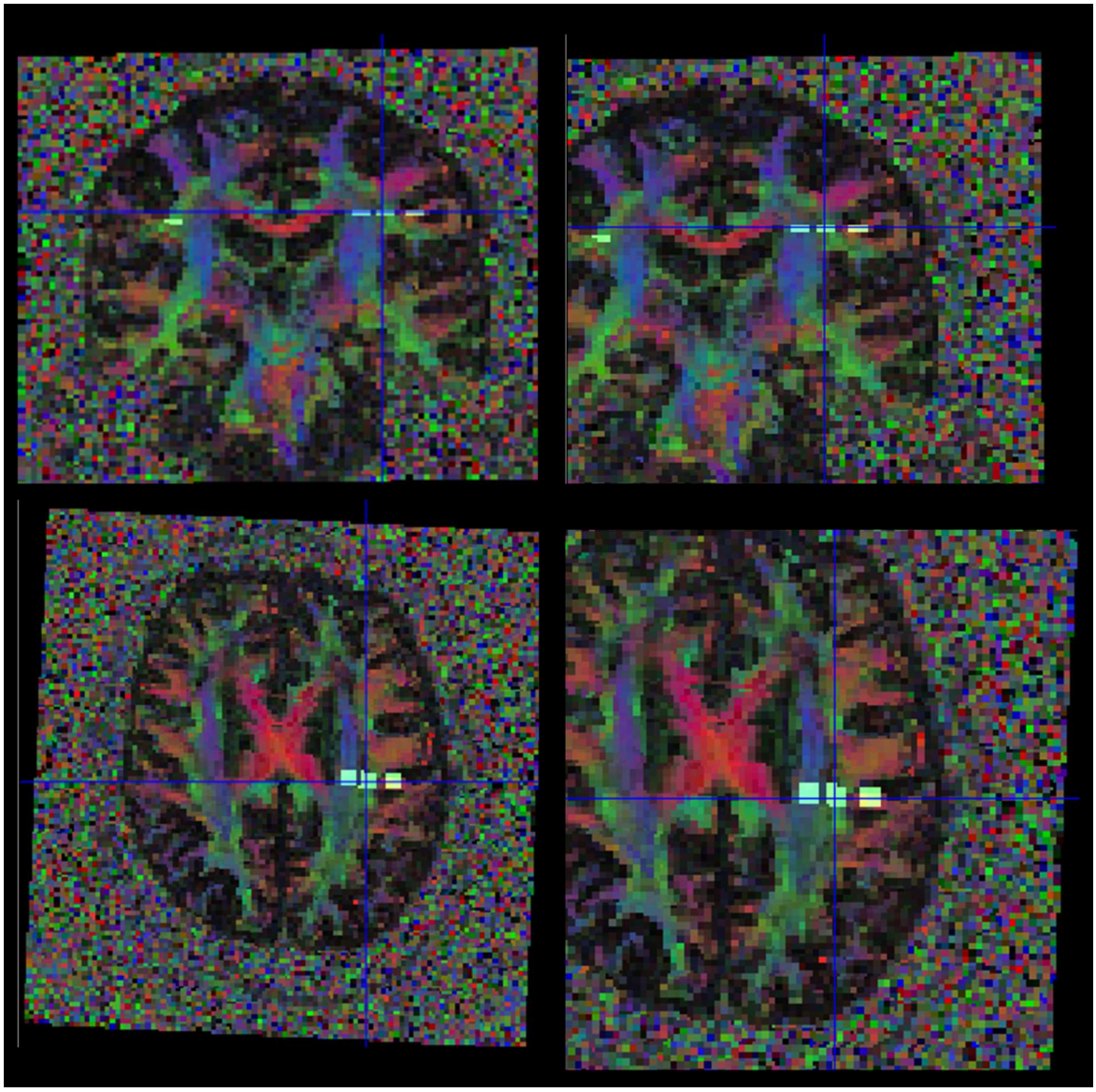

Figure F.a (A) Images in full volume, showing a misalignment of the regions-of-interest. (B) Magnification at 160x160 showing a better alignment.

(A) (B)

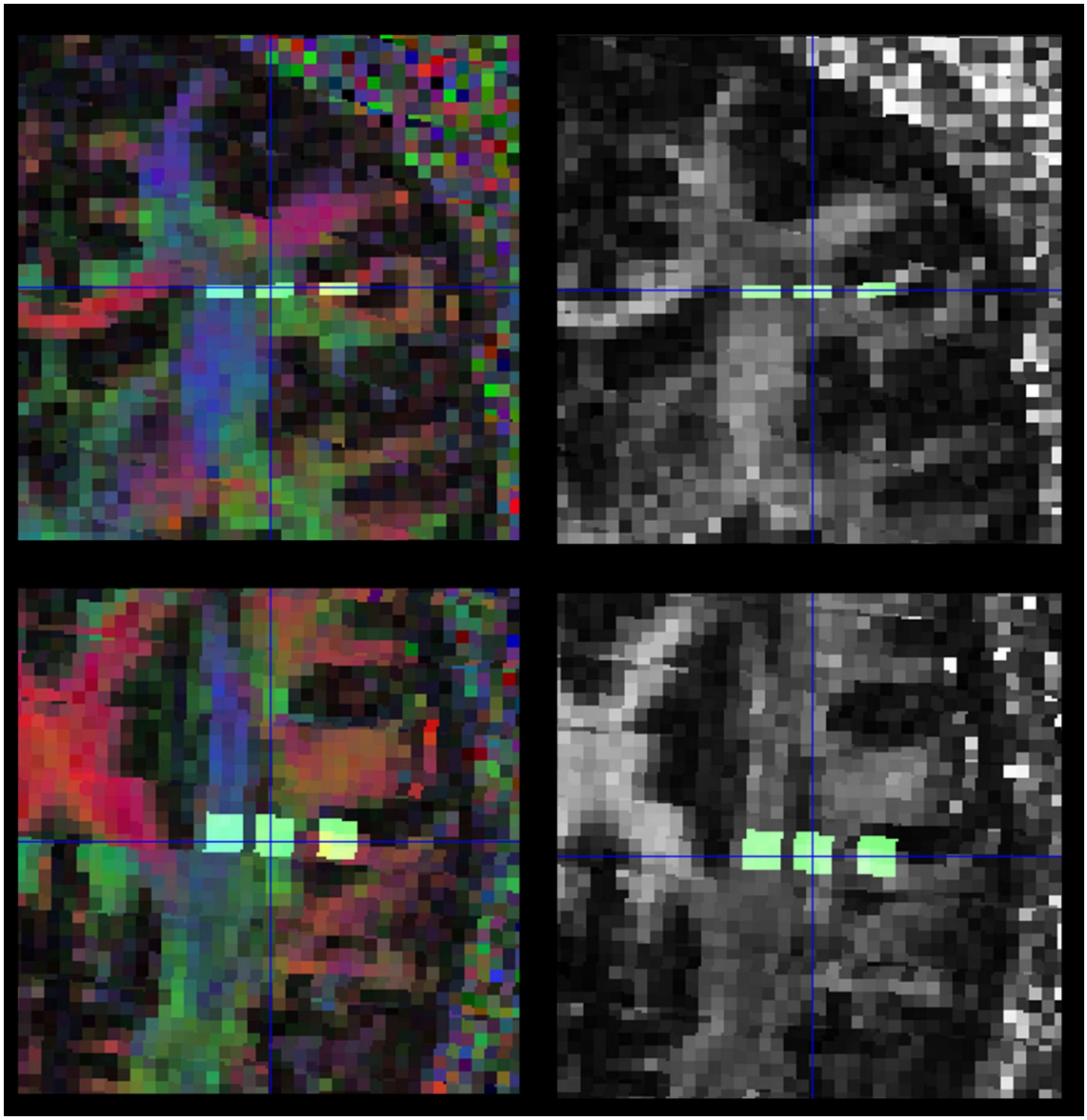

Figure F.b (A) Magnification at 80x80 showing the alignment of the regions-of-interest in the projection and association fibers. (B) Magnification at 80x80 using the near-neighbor interpolation for visualization.

Acknowledgements

First and foremost, I would like to express my gratitude to my thesis director, **Prof. Dr. Peter Schramm**, for his guidance and encouragement throughout this process. His insights and expertise have been invaluable in shaping this work.

I am also thankful to my co-supervisor, **PD. Dr. Jan Küchler**, for his expertise and constructive input, which significantly contributed to the direction and depth of this research.

My deepest thanks go to my thesis mentor, **Dr. Patricia Ulloa Almendras**, whose unwavering support, and patient mentorship have been crucial to the development of this dissertation. Her thoughtful collaboration and attention to detail were vital at every stage, and I am immensely grateful for her dedication.

I would like to acknowledge my colleagues, **Justus Rudolph, Aileen Schmidt, and Dr. Hannes Schwenke**, for their support and camaraderie. Special thanks to **Sherryl Sundell** for her help with language proofreading.

On a personal note, I owe my heartfelt thanks to my husband, **M.**, for his patience and perseverance in enduring this long journey with me. His steadfast support, even though the most challenging times, and his willingness to shoulder more than his fair share made it possible for me to complete this work.

Finally, my thanks go to my parents, whose encouragement has always been a source of strength, and to my son, **O.**, whose arrival brought new challenges and joys to this process. While he may not have made the work easier, he has certainly made life more interesting and meaningful.

To all these individuals, I extend my sincere gratitude for their invaluable contributions to this dissertation and the journey that led to its completion.